ACS Catalysis

Review

pubs.acs.org/acscatalysis

Carbon Materials as Catalyst Supports and Catalysts in the Transformation of Biomass to Fuels and Chemicals

Edmond Lam[†] and John H.T. Luong*[,‡]

[†]National Research Council Canada, Montreal Building, Montreal, Quebec, Canada H4P2R2

[‡]Irish Separation Science Cluster (ISSC), Department of Chemistry, Analytical and Biological Chemistry Research Facility (ABCRF), University College Cork, Cork, Ireland

ABSTRACT: Carbon plays a dual role as a catalyst or a catalyst support for chemical and enzymatic biomass transformation reactions due to its large specific surface area, high porosity, excellent electron conductivity, and relative chemical inertness. Advantageously, carbon materials can be prepared from residual biomass, an attractive property for decreasing the so-called "carbon-footprint" of a biomass transformation process. Carbon can be chemically functionalized and/or decorated with metallic nanoparticles and enzymes to impart or improve novel catalytic activity. Sulfonated porous carbon materials exhibit high reactivity in diversified catalytic reactions compared to their nonporous counterparts. However, the SO_3H groups prevent the incorporation of hydrophobic molecules into the bulk, thereby causing hydrophobic acid-catalyzed reactions to proceed only on the surface. Metal and enzymatic catalysts on carbon supports have significant advantages over other oxide materials for different types of reactions. The future success of biorefinery will require the design of a new generation of multifunctional catalysts, possibly derived from emerging carbon materials such as graphene, carbon nanotubes, and carbon monoliths, for the selective processing of carbohydrates and lignin. The most achievable and economical way is to convert lignocellulosic biomass directly, rather than pure cellulose, hemicellulose, or lignin using multifunctional catalysts.

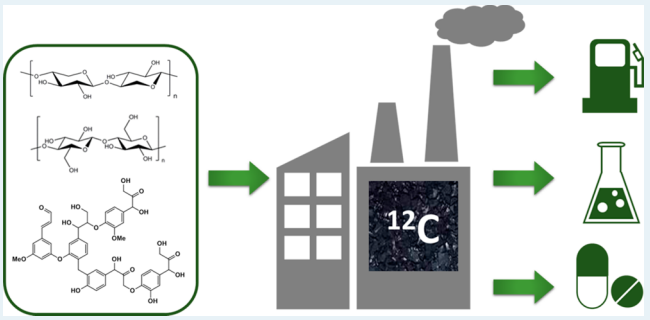

KEYWORDS: *carbon, graphene, nanotube, monolith, catalysis, catalyst, biomass, biocatalysis*

INTRODUCTION

Before the 19th century, trees and plants were the major source of energy and material feedstock. During the Industrial Revolution, coal became the primary substitute because of its abundant availability and ease of extraction from mining. However, by the 20th century, there was a major shift from coal to crude oil and natural gas due to lower production prices, abundance, simpler logistics, and broad-based conversion technology. Diversified, developed technologies enable the conversion of these petrochemicals into value-added plastics, detergents, and pharmaceuticals.[1] As an example, raw materials used in the German chemical industry are predominantly based on oil (76%), followed by gas and renewable raw materials (11%), and only 2% based on coal.[2] However, the excessive use of petrochemicals has created serious problems with respect to climate change, ecological impact, local economic dependencies, and sustainability.

Biomass derived from different sources includes lignocellulose, oilseed crops, sugar crops, starch crops, and aquatic cultures. Biomass materials also include biowastes from agricultural wastes, animal fats, urban and domestic wastes, and used plant oils. The most abundant lignocellulosic biomass consists of cellulose, hemicellulose, lignin, organic extractives and small amounts of inorganic materials. Roughly 40−45% content of dry wood is cellulose, a linear polymer of D-glucopyranose units linked by β-1−4 glucosidic bonds with crystalline and amorphous domains. About 25−35% content of dry wood is hemicellulose, a branched polysaccharide that bridges lignin to cellulose. The remaining content is largely lignin, a complex and heterogeneous amorphous polymer consisting of different phenyl propane units linked by ether and carbon−carbon bonds. Glucose monomers are obtained from the hydrolysis of cellulose as the main feedstock for the production of fuel alcohol or other chemicals by microbial conversion. Hemicellulose sugars are the substrates for the production of furfural and its derivatives, whereas lignin is a potential feedstock for higher value fuels and chemicals. Aromatic lignin is largely considered an agricultural waste product used for fuel with immature product applications.[3] Without new product streams, the lignin produced would flood the current world market for lignin used in specialty products.[4] *The old adage in the pulp industry has been that one can make anything from lignin except money.*

In 2010, the U.S. Department of Energy identified selected chemicals derived from biorefinery carbohydrates with potential commercial success through the integration of biofuels with

Received: June 16, 2014
Revised: July 21, 2014
Published: August 25, 2014

   dx.doi.org/10.1021/cs5008393 | *ACS Catal.* 2014, 4, 3393−3410

biobased products (Table 1).[5] However, the transformation of renewable biomass to such chemicals is not quick and simple, as each type of biomass must be treated in specific ways. Except for wood lignocellulosics, many biomass feedstocks are seasonal products that cannot be stored. The diverse variety of feedstocks poses a great challenge in the development of uniform conversion technologies.

Table 1. Bozell's Updated List of Potential Biobased Chemicals

biohydrocarbons	ethanol
furans	glycerol
3-hydroxypropionic acid	lactic acid
levulinic acid	sorbitol
succinic acid	xylitol

The discovery of new world shale gas reserves has put downward financial pressure on the conversion of biomass to chemicals.[6] Nevertheless, research in the development and implementation of efficient heterogeneous catalysts continues to grow.[7,8] Homogeneous Brønsted acids such as HCl, H_2SO_4, or H_3PO_4 are the predominant catalysts of choice for many biomass transformation reactions due to their relatively cheap commodity cost and availability. However, their corrosiveness, limited reusability and recovery, and disposal by neutralization often adds engineering complexity, energy usage, and extra cost to scale up processes for biorefineries. Many risks are associated with inadequate disposal of spent liquid acids into the environment, resulting in the use of extraordinary amounts of time and money to remediate affected areas. Strict government regulations have been a driving force for chemical producers to look for alternative feedstocks for biomass transformation reactions.

Carbon has been advocated as a leading material for chemical and enzymatic biomass transformation reactions due to its large specific surface area, high porosity, excellent electron conductivity, and relative chemical inertness. Advantageously, carbon materials can be prepared from residual biomass, an attractive property for decreasing the so-called "carbon-footprint" of a biomass transformation process. Carbon can be chemically functionalized and/or decorated with metallic nanoparticles (NPs) and enzymes to impart or improve novel catalytic activity. Based on the aforementioned properties, porous carbon materials are promising supports for heterogeneous catalysis compared to oxide supports. These oxide supports (TiO_2, γ-Al_2O_3, hydrotalcite, and mesoporous silica) are quite unstable in hot, pressurized water, a reaction condition commonly employed in many biomass transformation reactions.[8] The structural integrity of these materials begins to collapse, often resulting in decreased catalytic performance, product contamination as leached metals enter solution, and nonrecovery of catalyst material for subsequent reuse. The general aspect of carbon as catalyst supports has been addressed.[9] However, less attention has been paid to its role as a proper catalyst to transform biomass into chemicals that have attracted tremendous attention to establish a sustainable economy.

This review focuses on the catalytic conversion of biomass into chemicals using carbon as catalysts or catalyst supports. A recent review of Matthiesen et al.[8] identifies carbon as an organic–inorganic hybrid or carbocatalyst material for biomass transformation. We will examine the use carbon materials ranging from amorphous solids to nanostructured materials to create acidic carbocatalysts and metal NP/enzyme-supported materials. Special attention will be given to the functionalization of the carbon material with respect to the catalyst performance such as molecular diffusion of reactants, hydrogen spillover, and catalyst leaching. Carbon as electrode materials and/or electrocatalysts in fuel cell applications is not covered in this report.

GENERIC ASPECTS OF CARBON MATERIALS

Based on pore size, carbon materials are microporous (<2 nm), mesoporous (2–50 nm), and macroporous (>50 nm). Trimodal porous materials have all three levels of pores. Charcoal, diamond, and graphite are three well-known, naturally occurring carbon materials. The major carbon allotropes are summarized in Figure 1 based upon their hybridization state and atomic arrangement.

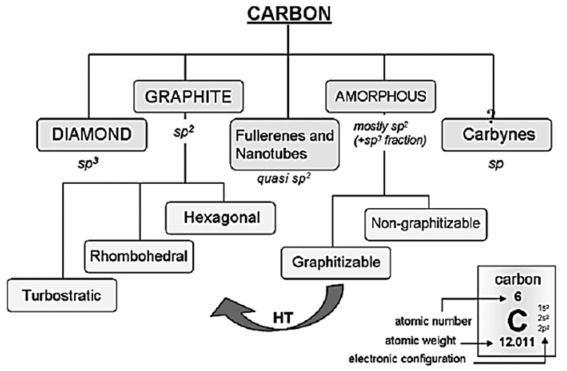

Figure 1. Allotropes of the element carbon. Adapted from ref 10.

High surface area activated carbon and carbon black are the materials of choice for most carbon-supported catalysts owing to their low cost and mass availability. Carbon black is an amorphous carbon prepared by the pyrolysis of organic polymers or hydrocarbon precursors at ~1500 °C. The residual elementary carbon atoms rearrange into stacks of flat aromatic sheets, which are cross-linked randomly with free interstices among them. Resulting carbon materials are composed with roughly planar layers of sp^2 hybridized carbons. The materials have a crystalline structure, but they are in the short-range and consequently lack stacking direction.[10] Activated carbon is prepared by physical or chemical activation. With physical activation, carbon materials are pyrolyzed at 600–900 °C in the absence of oxygen. Carbonized materials are then exposed to oxidizing atmospheres (oxygen or steam) at 600–1200 °C. In chemical activation, the raw material is impregnated with an acid, a strong base, or a salt (calcium chloride or zinc chloride), followed by carbonization at 450–900 °C. This route is preferred owing to the lower temperatures and shorter time needed for activating materials. Its structure is best described as a twisted network of defective carbon layer planes, cross-linked by aliphatic bridging groups. Activated carbon is an amorphous solid with an extraordinarily large internal surface area and pore volume.

Advanced science and engineering paves the way for the synthesis of various nanostructured carbon materials: (i) zero dimension (NPs); (ii) one dimension (carbon nanotubes); (iii) two dimensions (graphene sheets); and (iv) three dimensions (mesoporous carbons). Zero-dimensional carbon NPs can be

dx.doi.org/10.1021/cs5008393 | ACS Catal. 2014, 4, 3393–3410

produced from the hydrothermal carbonization of biomass to encapsulate metallic Pd cores for hydrogenation reactions.[11] Recent advances in carbon materials for biomass transformation reactions have focused on the use of one, two, and three-dimensional carbon materials. Carbon nanotubes (CNTs) are one-dimensional materials with a hollow geometry exhibiting large specific surface areas, good electrical conductivity, and excellent mechanical strength and thermal conductivity.[12] Multiwalled CNTs (MWCNTs) are metallic, whereas single-walled CNTs (SWCNTs) are semiconductive, depending on their helicity and diameter which can greatly affect charge transfer processes. CNTs serve as ideal and unique templates for metallic NP immobilization/deposition to form nano-architectures as attractive supports for heterogeneous catalysts. Two-dimensional graphene has emerged as a new kind of catalyst support material due to its unique physicochemical properties as described for CNTs. Together with a remarkable surface area of 2630 m^2/g for a single layer,[13] graphene exhibits a strong interaction with bimetallic NPs such as Au, Ni, Co, and Pd.[14−16] Graphene can also be functionalized with polymers,[17] doped with nitrogen, conjugated with different functional groups to impart varying electronic and acid properties, and strategically dispersed with metal NPs for catalytically active facet sites.[18,19]

A variety of three-dimensional carbon porous materials have recently garnered special attention as catalyst support materials. Templating using hydrocarbon gels is a proven method for producing high surface area, porous carbon materials. Starbon, mesoporous carbon materials with tunable surface chemistry derived from starch, is produced via a three-step process involving gelation of a starch network, solvent evaporation to form a mesoporous structure, followed by the treatment with organic acid and pyrolysis (Figure 2).[20−22] Starbon materials typically have surface areas of 150−600 m^2/g and pore sizes between 7 and 17 nm.[23] Structured carbon supported catalysts exhibit higher activity and stability than the corresponding bulk oxide material associated with certain favorable metal−carbon interactions involving oxidized carbon surfaces or $\pi-\pi$ functionalities on the carbon support.[24] Otherwise, only limited interactions associated with the pristine basal plane inhibit functionalization as observed in the atomic layer deposition of metals on pristine carbon.[25]

Carbon aerogels are nanostructured carbons obtained from the carbonization of organic aerogels prepared from the sol−gel polycondensation of certain organic monomers. These materials have a macroscopic form with nanoscopic pore texture. Thus, the surface area, pore volume, and pore size distribution are tunable, depending upon the synthesis and processing conditions. Carbon aerogels can be formed into monoliths, beads, powders, or thin films.[26] Carbon monoliths have high specific surface areas, uniform and tunable 3D interconnected porous structure, good chemical and thermal stability. These properties usually lead to several distinct advantages such as high flow-through permeability, rapid heat-mass transfer, good electronic conductivity, high molecular interaction efficiency and ease of handling.[27,28] Carbon monoliths can be fabricated by hard template[29] via replicas from colloidal crystals or silica spheres,[30] and silica monoliths.[31] A carbon source is introduced to the void of inorganic templates by impregnation, infiltration or chemical vapor deposition to form a carbon/template precursor. Carbonization under controlled temperature and inert gas flow creates carbon monoliths. Metal elements are then removed from the template

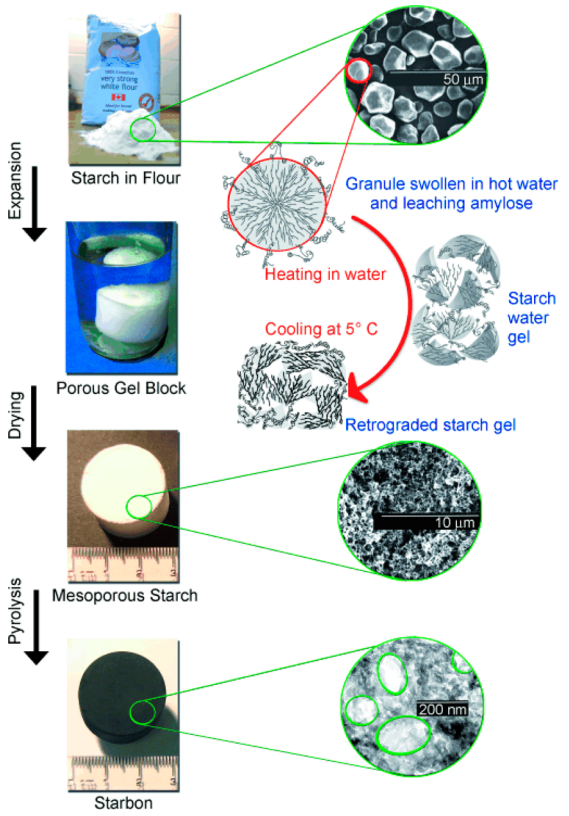

Figure 2. Synthesis of Starbon. Reproduced from ref 20.

with alkaline or HF solutions if required. An alternative approach is based on a soft template[32,33] such as self-assembled copolymer templates, colloidal crystal templates, a combination of both hard and soft template for tailoring macro- and mesopores.[34] Both hard and soft template approaches are quite successful but require multiple time-consuming steps. Template-free procedures using a mixture of phenol resin and ethylene glycol can be formed[35] by pyrolyzed at >500 °C to become monoliths.[36]

CARBON MATERIALS AS CATALYST SUPPORTS

The ensemble of a catalyst and its support can be regarded as an entirety (i.e., supported catalyst). Important properties of the support material include mechanical strength, pore distribution, chemical and thermal stability. Catalyst supports can be inert or active in reactions, and in some cases, they might act as a stabilizer to prevent the agglomeration of lower-melting-point materials or serve as a reservoir for semi molten salts. The supports can cooperate with the catalysts to promote simultaneous and mutually beneficial reactions.

Carbon materials are a popular choice because they can be fabricated in different physical forms and shape. Table 2 shows some of the key advantages of using carbon support materials for catalysts, and Table 3 compares the physical properties of the most commonly employed carbon materials.

Oxygen surface groups are of great interest in the preparation of carbon-supported catalysts, because the most common procedure is still contacting the carbon support with an excess catalyst precursor. Carbon-based materials are still the most practical for the preparation of noble metal catalysts,[37] particularly for Pt-based catalyst.[38] The distribution of Pt on the carbon support surface depends on the solvent used for

dx.doi.org/10.1021/cs5008393 | ACS Catal. 2014, 4, 3393−3410

Table 2. Key Advantages of Carbon Support in Catalytic Applications

1. resistance to acidic or basic media
2. tailored pore size distribution for specific reactions
3. amphoteric character due to the presence of various oxygenated functional groups which enhances metal adsorption and catalyst dispersion
4. the structure is stable at high temperatures (even above 1000 K); except in the presence of oxygen >500 K and for hydrogenation reactions >700 K
5. less expensive compared to alumina and silica supports; porous carbons can be prepared in different physical forms (granules, extrudates, pellets, fibers, cloths, etc.).
6. hydrophobic carbon can be modified to increase the hydrophilicity
7. active phase can be recovered by eliminating the support through burning away the carbon

impregnation. The chloroplatinic acid precursor is mostly located at the particle external surface when using water, but it readily penetrates into the interior of the pores when using acetone, resulting in a more uniform distribution of metal throughout the carbon structure.[39] The carbon-Pt precursor interaction is favored by the presence of oxygen surface groups where a hydrophilic carbon surface facilitates better dispersion of the Pt precursor. Activated carbon and carbon black have served as catalyst supports for many reactions. In particular, commercially available carbon black (e.g., Vulcan XC72) is most commonly used for Pt and Pt-alloy catalysts owing to its high conductivity and low cost. However, thermochemical instability and corrosion are frequently encountered in fuel cell applications using these types of catalysts. The role of carbon as the support is not merely that of a carrier; indeed, it can sometimes contribute to catalytic activity (hydrogen spillover) and reacts to some extent with other catalysts during the catalytic process.[40]

CARBON MATERIALS AS CATALYSTS

Liquid acids such as H_2SO_4, HCl, H_3PO_4, various carboxylic acids, and *p*-toluenesulfonic acid are often used for the hydrolysis or polycondensation of biomass in the production of glucose, xylose, and other chemicals. In general, H_2SO_4 has been the most frequently used in the hydrolysis of lignocellulosic biomass at 363−533 K and under atmospheric or higher pressure. With dilute acid solution, higher temperature and longer reaction time are required.[41] In contrast, the hydrolysis reaction is feasible in a short reaction time with concentrated acid. However, the use of concentrated acid solutions could lead to a decrease of the yields of glucose and xylose due to complete degradation of the monomeric sugars. Despite their low price, the implementation of these acids requires significant cost in separation, reuse, and treatment of salt wastes. These problems could be circumvented if carbonic acid, prepared from CO_2 and water, can be used as a catalyst.[42] However, this "so-called" green process must use pressurized CO_2 at 533 K.[43]

Carbon materials exhibit an acid−base character owing to several types of oxygen functionalities (Figure 3). They can be

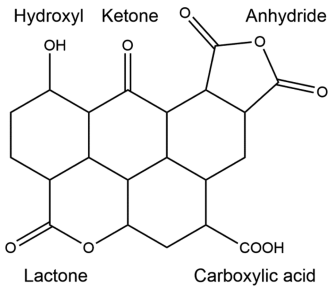

Figure 3. Some types of oxygen surface groups in activated carbon.

prepared by functionalizing the carbon surface with acids or bases. Amorphous carbon bearing SO_3H groups as an insoluble Brønsted acid is available for various acid-catalyzed reactions (Figure 4).[44] Solid catalysts are easily separated from the liquid

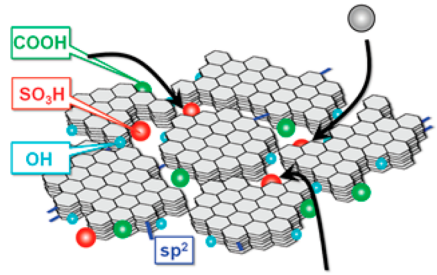

Figure 4. Schematic structures of proposed SO_3H-bearing CCSA materials carbonized below 723 K. Adapted from ref 44.

mixture after the reaction, enabling their possible reuse and continuous processing via a flow fixed-bed reactor in the catalytic hydrolysis of lignocellulosic biomass.[45−48]

Carbons produced from thermal carbonization of aromatic compounds or carbohydrates provide an inexpensive source of carbon materials for the production of so-called "sugar catalysts". Carbonization is performed at 200−300 °C followed by refluxing with sulfuric acid to generate the active sulfonic functional groups.[49,50] Sugar catalysts possess a graphene-like structure containing 1.2−1.3 nm aromatic groups with a surface area of <5 m^2/g.[44] Several functionalized graphene sheets accumulate to form flexible domains that are linked together to form catalyst particles (typically 10−40 mm diameter). The

Table 3. Comparison of Carbon Materials for Catalyst Supports

carbon material	specific surface area (m^2 g^{-1})	pore volume (cm^3 g^{-1})	density (g cm^{-3})	electrical conductivity (S cm^{-1})	cost
graphite	10−100	0.01−0.1	2.26	104	low
activated carbon	1000−3500	0.6−2	0.4−0.7	0.1−1	low
templated porous carbon (includes Starbon, carbon monoliths)	500−3000	0.7−2	0.5−1	0.3−10	high
carbon fibers	1000−3000	0.3−0.7	0.3−0.8	5−10	medium
carbon aerogels	400−1000	2−6	0.5−0.7	1−10	low
CNTs	120−500	2.5	0.6	10^4−10^5	high
graphene	1500−2500	2−3.5	>1	106	high

dx.doi.org/10.1021/cs5008393 | ACS Catal. 2014, 4, 3393−3410

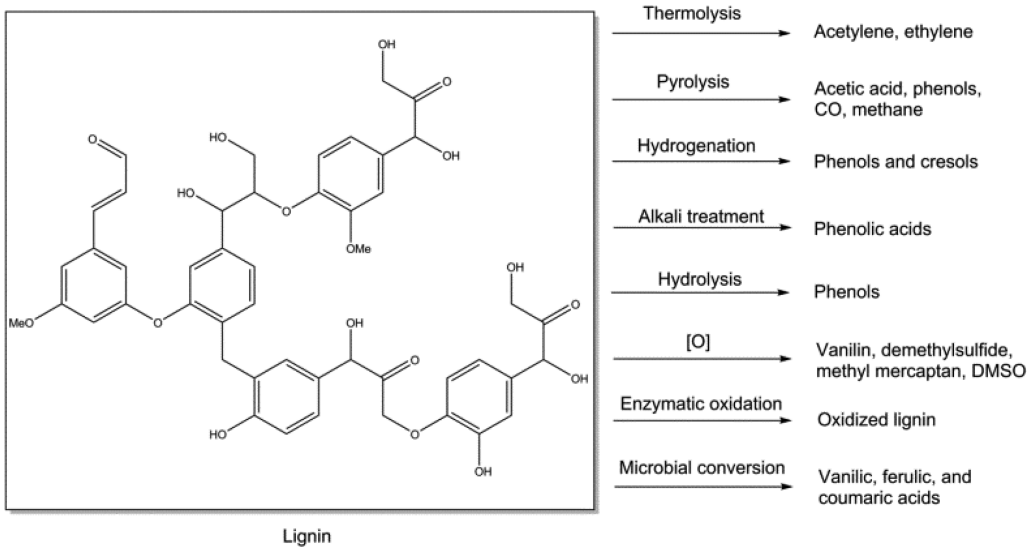

Figure 5. Transformation products of lignin.

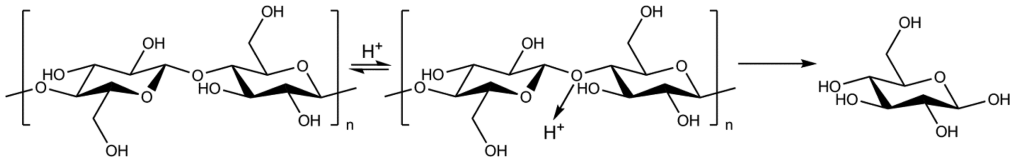

Figure 6. Cellulose hydrolysis to glucose.

carbon materials have SO_3H groups with a Hammett acid strength (H_0) of −8 to −11, comparable to that of concentrated H_2SO_4.[51]

A sulfonated porous carbon catalyst with a specific surface area of 1560 m^2/g is prepared by the carbonization of $ZnCl_2$-impregnated wood powder followed by sulfonation.[52] The porous carbon catalyst carbonized at above 723 K contains high densities of micro- and mesopores. A variety of products could also be derived from lignin (Figure 5), of which several could be attained through activation of selective lignin bonds. Activated carbon and acidic sulfonated carbon, produced from lignin, are excellent catalysts for hydrolysis/dehydration of polysaccharides and polyols.[53]

Templated porous carbon materials such as carbon monoliths are excellent candidates for solid acids because of high mechanical strength, large volumetric adsorption capacity, and ease of transport. Active carbon monoliths (ACM) with high specific areas (950 m^2/g) are commonly prepared by impregnation of porous ceramic with a carbonaceous solution or simply by the activation of biomass with H_3PO_4 and $ZnCl_2$. Surface modification of carbon monoliths by oxidation,[54] KOH treatment,[55] and amination[56] are feasible by adapting the procedures developed for activated carbon, carbon black, glassy carbon, and so forth. Carbon monoliths are subjected to a strong oxidizer (HNO_3, H_2O_2, permanganates, and dichromates, etc.) or oxidizing gases (air, oxygen, ozone, nitrous oxides, etc.) to introduce oxygenated functional groups comprising carboxylic acids, esters, ketones, phenols, lactones, lactols, or quinones.[57] Porous carbon materials functionalized with sulfonic acid groups have low cost, high stability, and acidic activity. It is possible to fabricate these materials by one-pot hydrothermal carbonization of a mixture of *p*-toluenesulfonic acid/glucose/resorcinol at 180 °C.[58]

BIOMASS TRANSFORMATION BY CARBON CATALYSTS AND CARBON SUPPORTED CATALYSTS

Carbon catalysts and carbon-supported catalysts can facilitate a variety of reactions for the catalytic conversion of biomass feedstocks into chemicals. Often, multifunctional catalysts are designed to catalyze more than one type of reaction (for example, dehydration by acid groups on carbon support, followed by hydrogenation on metal NP) to allow for highly efficient conversion of feedstocks into the platform molecules that could achieve commercial success through the proper integration of biofuels with biobased products.

Hydrolysis. Crystalline pure cellulose is not hydrolyzed (Figure 6) by conventional strong solid Brønsted acid catalysts including H-mordenite, Nafion, and Amberlyst-15. However, amorphous carbon bearing SO_3H, COOH, and OH groups functions as an efficient catalyst for the reaction.[59] The 110 kJ/mol activation energy of the carbon catalyst is lower than 170 kJ/mol of H_2SO_4 for the hydrolysis of cellulose into glucose. The catalyst performance is attributed to its ability to adsorb 1,4-glucan, as measured by liquid chromatography, in comparison with the other solid acids. A broadband at 2300−2700 cm^{-1} in the FTIR was assigned to the strong hydrogen bond between SO_3H groups indicative of hydration tolerant SO_3H groups in the carbon material.

The theme of substrate adsorption to promote the hydrolysis of water-soluble β-1,4-glucan was reported for a carbon-based solid acid, amorphous carbon containing graphene sheets bearing SO_3H, COOH, and phenolic OH groups.[60,61] The turnover frequency (TOF) of SO_3H groups in the carbon material exceeds 20 times those of the conventional solid acids (Nafion NR50, Amberlyst-15 and niobic acid). A synergistic effect between phenolic OH or COOH groups in the carbon

dx.doi.org/10.1021/cs5008393 | ACS Catal. 2014, 4, 3393−3410

material, and SO_3H groups bonded to the carbon therefore function as effective active sites for both decomposing the hydrogen bonds and hydrolyzing the β-1,4-glycosidic bonds in the adsorbed long chain water-soluble β-1,4-glucan aggregate.

The optimal hydrolysis conditions can be established using an artificial neural network (ANN) and a response surface methodology (RSM) to decipher the novel solid−solid interface catalysis and the role of water.[62] The correlations of the reaction and each parameter are discussed on the basis of the reaction mechanism, ANN, and RSM. A sulfonated activated-carbon catalyst shows a remarkably high yield for glucose due to the high hydrothermal stability and the excellent catalytic property, the features of the strong acid sites of SO_3H functional groups, and the hydrophobic planes.[63] Similar optimization studies are performed for the corn starch saccharification using the sulfonated carbon catalyst by an analysis of variance (ANOVA) and an ANN model.[64]

The starting carbon material for sulfonation might have a profound impact on the catalyst performance. For example, sulfonation of partially carbonized polyvinyl chloride in fuming H_2SO_4 produces a material with sulfonated carbon sheets linked by flexible aliphatic hydrocarbons as opposed to typical sulfonated activated carbon with rigid sp^2 bonds (Figure 7).

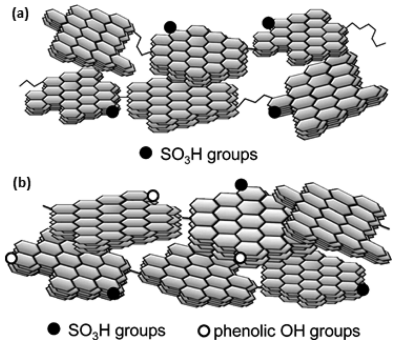

Figure 7. Structure of (a) PVC-activated carbon and (b) cellulose-derived activated carbon. Adapted from ref 65.

The hydrolysis of cellobiose is improved by virtue of the increased diffusion of reactants and enhanced reactivity of SO_3H groups bonded to the carbon sheets.[65] Of interest is the preparation of an amorphous carbon-based catalyst by sulfonation of the biochar obtained from fast pyrolysis of biomass in nitrogen at 550 °C.[66] The sulfonated carbon catalyst with acidity of 6.28 mmol/g converts cellulose in methanol at moderate temperatures to α, β-methyl glucosides (90% yield) in short reaction times.

Sulfonated CMK-3 (ordered mesoporous carbon) is used for the hydrolysis of cellulose with a conversion of 94.4% and a glucose yield of 74.5%.[67] Increasing the temperature from 150 to 300 °C increases the acid density, but the specific surface area reaches a maximum at 250 °C. Mesoporosity affects the glucan adsorption as observed for mesoporous carbon NPs (MCN).[68] MCN adsorbs 303 mg of long chain glucans/g of MCN compared to graphite-type carbon nanopowders (CNP) with 7.7 mg of long chain glucans/g of CNP. The glucan adsorption on CNP is significantly lower due to its low internal mesoporosity because this material has a higher external surface area relative to MCN. Sulfonated MCN materials, with 90% weak acid sites and 1.6 nm pore sizes, can depolymerize xylan to xylose.[69] However, only a fraction of weak-acid surface sites (determined by acid−base back-titration) at high local concentrations at the surface are catalytically active, consistent with the hydrolysis of chemisorbed glucans on inorganic-oxide surfaces.[70]

A carbon-supported Ru catalyst enhances the hydrolysis of cellulose to glucose and then hydrogenates glucose to sugar alcohols (sorbitol and mannitol) in H_2 at 0.7−0.9 MPa.[71] A mix-milling pretreatment of cellulose and the Ru catalyst together selectively accelerate the hydrolysis step in 68% yield. The addition of acids in the cellulose conversion is less effective as a result of promotion of side-reactions. Similarly, a mechano-catalytic approach combining impregnation of cellulosics with 0.5 M H_2SO_4, mechanical ball milling and hydrogenolysis over Ru/C catalysts, is used for the production of C4−C6 sugar alcohols with yields of up to 94% for hexitol from glucose.[72] The corrosion of the ball-milling apparatus and the recovery of the H_2SO_4 are two issues of this process. Cellulose can also be converted to C2−C6 polyols by using the Ru/CNT catalyst in the presence of hydrogen.[73] This conversion follows a two-step process; cellulose is hydrolyzed by acid-functionalized CNTs into reducing sugars followed by hydrogenation by Ru to sugar alcohols. The sorbitol yield increases with decreasing crystallinity of the carbon support.

Another example of a multifunctional catalyst is a tungsten carbide NP supported on a high surface area, three-dimensional mesoporous carbon (MC) for the direct conversion of cellulose to ethylene glycol at 72.9% efficiency.[74] The reaction combines the hydrolysis of cellulose and hydrogenation/hydrogenolysis of cellulose-derived sugars to produce the final polyol. The MC was prepared by a nanocasting method with sucrose as the carbon precursor, and a hard template consisting of commercial silica and SBA-15. The MC has advantages of good accessibility of the mesopores to allow the molecular diffusion of the reactant and products from the active sites compared to microporous activated carbon. Similarly, a Pt catalyst supported on a sea-urchin-like three-dimensional mesoporous carbon was used for the hydrolytic hydrogenation of cellulose to hexitol in 80% yield (Figure 8).[75] Like the previous example, N_2 adsorption−desorption isotherms show a very large surface area of 1570 m^2/g with a mesoporous area of 1340 m^2/g. Abundant oxygen groups on the carbon support facilitate the transport of cellulose to the active sites within the mesopores. Furthermore, the Pt NPs not only hydrogenates glucose to hexitol, but also induces hydrolysis via a hydrogen spillover effect.

The conversion of biomass-derived carbohydrates into furanic aldehydes such as furfural and 5-hydroxymethylfurfural (HMF) has attracted considerable attention as they are important intermediates for the production of biofuels and high value-added chemicals.[76] Furfural is derived from C5 sugars (Figure 9), whereas HMF is synthesized by the dehydration of C6 carbohydrates, including monomeric and polymeric carbohydrates such as glucose, fructose, and cellulose (Figure 10 and Figure 11). Levulinic acid, a further downstream acid hydrolysis product of HMF, can be transformed to other value-added chemicals (Figure 12). Various strategies have been developed to overcome low yields attributed to byproduct formation and product separation from reaction mixtures with limited scalability at industrial levels.[77−79]

Graphene, graphene oxide, sulfonated graphene, and sulfonated graphene oxide (SGO) have been prepared, characterized, and tested for the dehydration of xylose to furfural in water. In particular, SGO is proven as a rapid and water-tolerant solid acid catalyst even at very low catalyst

dx.doi.org/10.1021/cs5008393 | ACS Catal. 2014, 4, 3393−3410

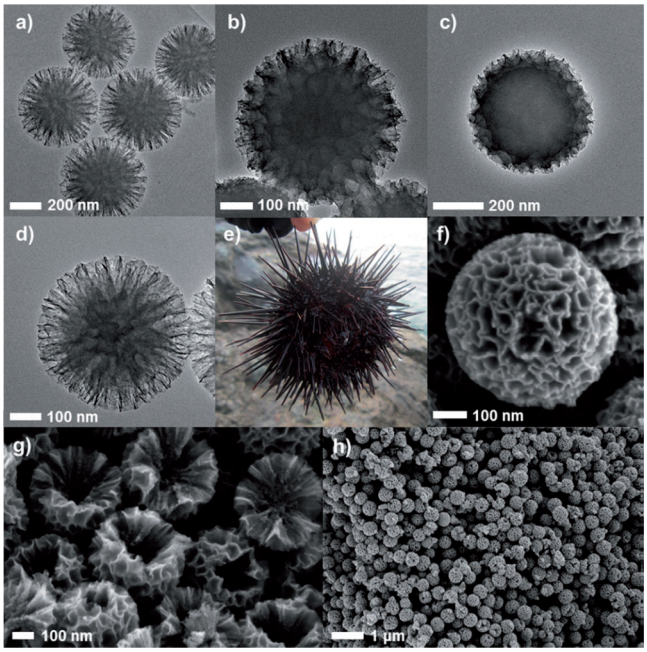

Figure 8. FHR-TEM images of (a) silica template, (b) silica−carbon composite after drying, (c) silica−carbon composite after aging, (d) sea-urchin-like three-dimensional carbon, (e) image of sea urchin *Echinometra mathae*. SEM images of (f) single sea-urchin-like three-dimensional carbon, (g) cross-section of three-dimensional carbon, and (h) prepared three-dimensional carbon particles in a large-scale view. Adapted from ref 75.

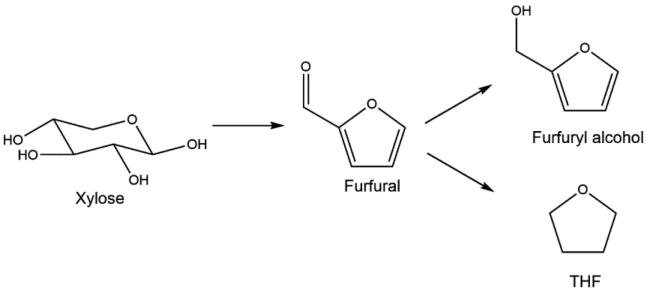

Figure 9. Conversion of xylose to furfural-derived chemicals.

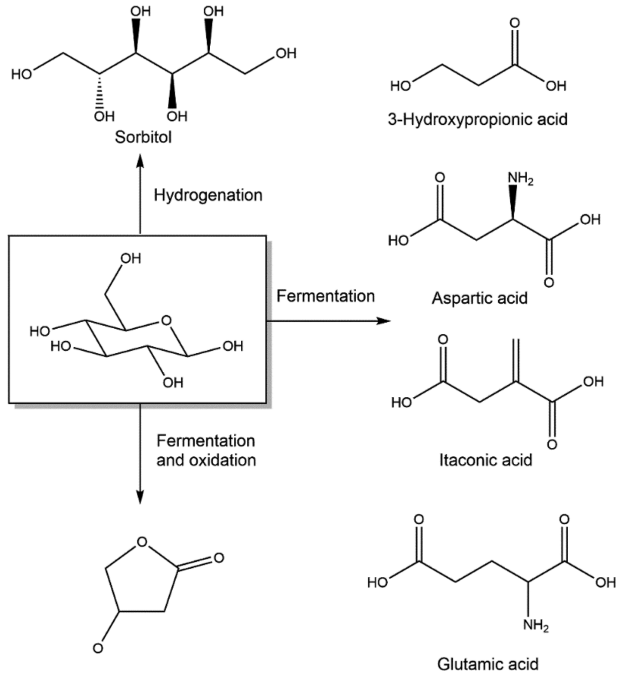

Figure 11. Glucose conversion products.

loadings down to 0.5 wt % versus xylose, maintaining its initial activity after 12 tested repetitions at 200 °C, with an average yield of 61% versus 44% for the uncatalyzed system.[80] The covalently bonded aryl sulfonic acid groups are the key active sites for high-temperature production of furfural in water. They are more acidic and thermally stable (confirmed by TGA and FTIR) under the reaction conditions than other surface functional groups attached to the graphene surface. Titanium dioxide NPs (8−9 nm) deposited on reduced graphene oxide or carbon black by microwave efficiently catalyze the aqueous-phase dehydration of xylose into furfural at 170 °C with high furfural yields (67−69%) at high conversions (95−97%).[81] The catalytic performance is not significantly affected by the type of carbon supports, suggesting that cheap amorphous carbons can be used to support titania NPs.

Amorphous carbons are produced by hydrothermal carbonization of cellulose at 250 °C for 4 h (Figure 13). The

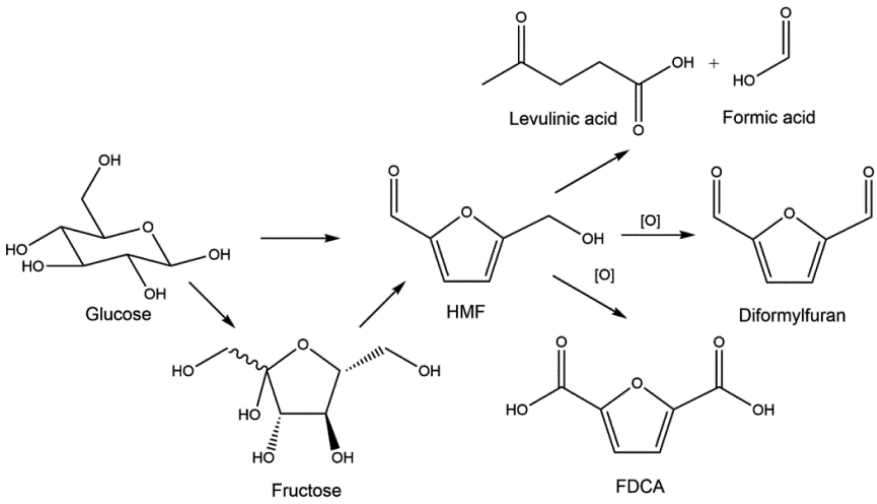

Figure 10. Conversion of glucose to different HMF-derived chemicals.

dx.doi.org/10.1021/cs5008393 | ACS Catal. 2014, 4, 3393−3410

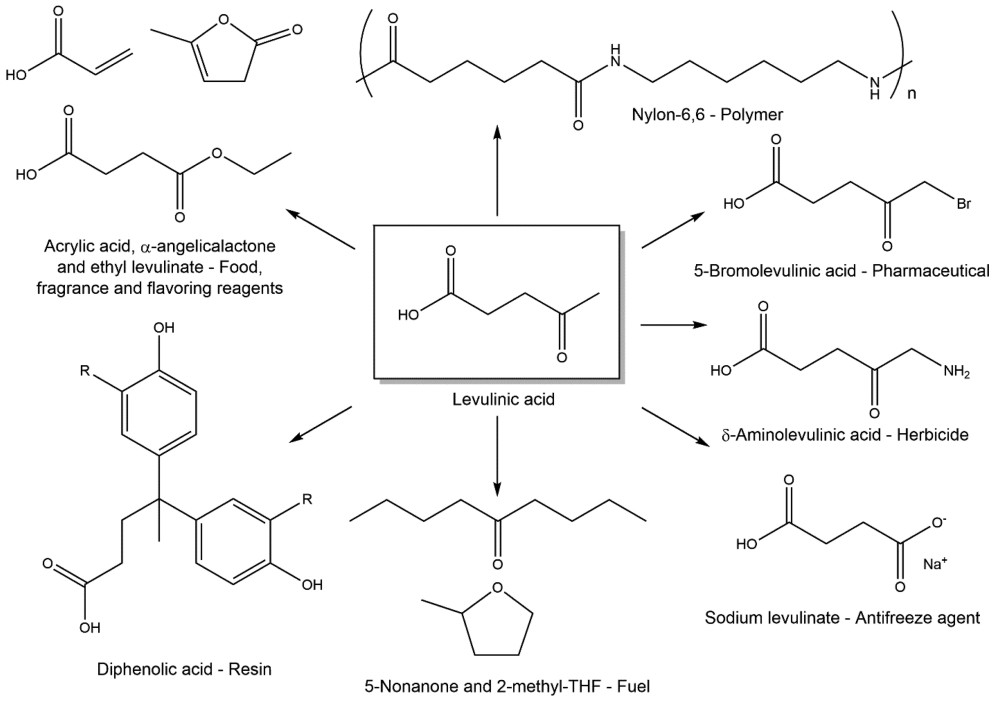

Figure 12. Transformation of levulinic acid to other products.

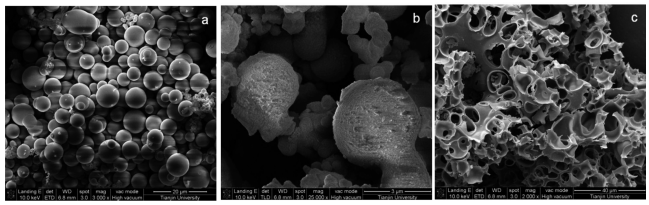

Figure 13. Typical SEM images of carbon materials obtained by hydrothermal treatment of cellulose: (a) product without post-treatment, carbonaceous solid (CS); (b) product with H_2SO_4 post-treatment, carbonaceous sulfonated solid (CSS); and (c) product with KOH and H_2SO_4 post treatment, activated carbonaceous sulfonated solid (a-CSS). Adapted from ref 82.

treatment of the carbonized cellulose with H_2SO_4 at 200 °C produces a carbonaceous sulfonated solid (CSS), equivalent to an acid concentration of 0.953 mmol/g and a low surface area of 0.5 m^2/g. Acid content was confirmed by inductively coupled plasma mass spectrometry and elemental analysis. Conversely, when the carbonized cellulose is first treated with KOH, followed by sulfonation, a high surface (514 m^2/g) but low acidity (0.172 mmol/g) material (a-CSS) results. Both materials have been tested for the dehydration of fructose to 5-HMF in ionic liquids with CSS achieving a higher yield of 83% yield (at 80 °C within 10 min) in comparison to <70% for a-CSS, implying a higher influence of acidity on the fructose hydrolysis than the surface area.[82]

CNTs and carbon nanofibers (CNFs) functionalized with poly(*p*-styrenesulfonic acid) and benzenesulfonic acid groups are tested for the conversion of fructose to 5-HMF. A linear correlation between acid site density and fructose conversion is observed. However, the catalytic activity drops from 84% yield to 69% after five successive reactions at 120 °C.[83] HMF and furfural are produced from cassava waste using a sulfonated carbon-based catalyst in an acetone-DMSO mixture (70/30% w/w) and water at a ratio of 10/90% w/w.[84] The catalyst is highly stable and typical reaction conditions are 250 °C and 1 min, with a mass loading corresponding to a weight ratio of 0.05:1 (catalyst to cassava waste). Alternatively, self-assembled nanoparticulates of porous sulfonated carbonaceous TiO_2 containing a 1.2 ratio of Brønsted to Lewis acidic sites for hydrolysis are also effective catalysts for the production of HMF and furfural from saccharides in a biphasic solvent of water and methyl-THF.[85]

Hydrogenation. One important consideration in heterogeneous hydrogenation catalysis is the phenomenon called "hydrogen spillover" in which a support material can become catalytically active as the dissociative absorption of hydrogen atoms migrates from a metal NP surface to the support surface.[86] The hydrogenation reaction rate is the sum of the reaction rates on both the metal and support surface, where the rate can be faster on either the metal NP or support surface. The spillover effect is often promoted by the presence of oxygen-bearing groups (carboxyl and hydroxyl groups) on the carbon surface.[87] In fabricating metal NP-supported materials, the presence/absence of surface oxygen groups will dictate the possible electrostatic interactions between the sites on the carbon surface and metal cations or anions as below:

(i) Oxidation of the carbon typically renders the carbon surface more acidic and thus negatively charged over a wide range of pH. This surface exhibits electrostatic repulsion of metal anions, e.g., $PtCl_6^{2-}$ but favors electrostatic attraction of metal cations, e.g. $Pt(NH_3)_4^{2+}$.
(ii) Increasing the basicity on the basal plane surface of oxygen-free carbon favors the electrostatic attraction with the metal anion (e.g., C_π-H_3O^+-$PtCl_6^{2-}$) and also reduces the electrostatic repulsion (e.g., COO^--$PtCl_6^{2-}$).
(iii) C═O groups acting as anchoring centers hinder agglomeration and surface diffusion of catalyst particles across the graphene layers.

The surface chemistry of the supporting material will effect metal NP dispersion and hydrogen spillover. The cumulative

dx.doi.org/10.1021/cs5008393 | ACS Catal. 2014, 4, 3393−3410

effects can be beneficial or detrimental to a hydrogenation reaction. For example, a case of beneficial effect is the direct conversion of sorbitol from cellulose. Pt nanocatalysts loaded on reduced graphene oxide (Pt/RGO) are prepared by a convenient microwave-assisted reduction approach with ethylene glycol as reductant.[88] The conversion of cellulose or cellubiose into sorbitol at 91.5% and 58.9%, respectively, is highest for RGO compared to other solid supports tested. The catalytic activity can be attributed to the appropriate Pt particle size and the hydrogen spillover effect of the Pt/RGO catalyst. The catalytic performance initially increases, then decreases with increasing particle sizes up to 3.6 nm, which could be regulated by controlling the microwave temperature. It was noted that overoxidation of the carbon support could decrease the rate of hydrogenation. In a detrimental case, the hydrogenation of dinitrotoluene did not improve in Pd/C catalysts where the support material was oxidized with HNO_3, despite increased Pd dispersion and a detected hydrogen spillover effect, as determined by oxygen−hydrogen titration.[89] The dispersion of Pd into unfavorable micropores and the presence of hydrophilic carbon surfaces may prevent larger nonpolar reactant molecules from accessing reactivity sites on the catalyst surface.

Platform molecules with multiple functionalities, like succinic acid, are transformed into a variety of high value chemicals through chemical transformation. The conversion of succinic acid to diester and cyclization derivatives is a strategic step in the manufacture of special polymers and chemicals (Figure 14).

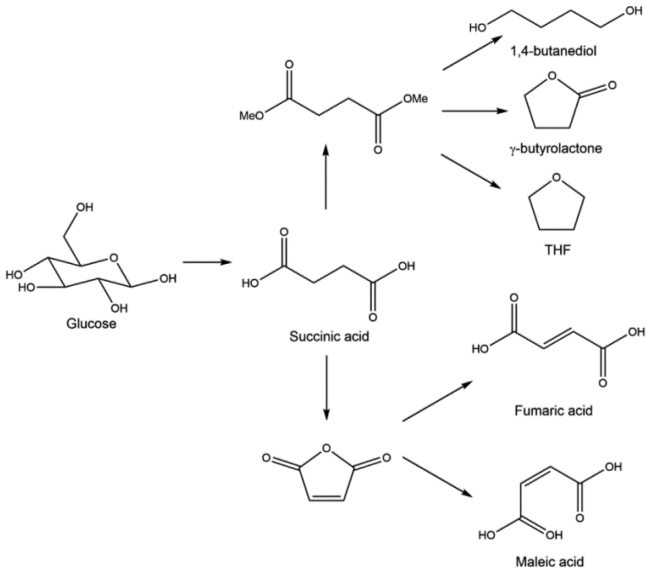

Figure 14. Succinic acid transformations.

Succinic acid can be hydrogenated to γ-butyrolactone, THF, and 1,4-butanediol, three solvents commonly used as precursors for downstream chemicals. Pd, Pt, Ru, and Rh NPs are deposited on Starbon by H_2 reduction and tested for the hydrogenation of succinic acid in aqueous ethanol at 10 bar of H_2 and 100 °C.[90] Ru−Starbon-300 presents the highest conversion (90%) and selectivity (60%) toward tetrahydrofuran. Pt−Starbon-300 enables the synthesis of 1,4-butanediol with 78% conversion and 85% selectivity. γ-Butyrolactone is obtained at 45% conversion of succinic acid, with 65% selectivity using 5% Pd−Starbon-300. Inductively coupled plasma atomic emission spectroscopy (ICP-AES) was used to confirm that the metallic NPs did not leach from the catalyst after reaction, as corroborated by their XPS data.

D-Xylitol is produced from D-xylose through catalytic hydrogenation using a nickel catalyst at 80−140 °C and pressure up to 50 atm.[91] For xylan as the substrate, the conversion yield is 50−60%. Pt NPs (1.3 nm) on MWCNTs are used for the hydrogenation of xylose to xylitol with 100% conversion of xylose and 99.3% selectivity to xylitol, compared to commercial Pt/C, Ru/C, and Raney Ni catalysts.[92] Compared to the commercial Pt/C, the catalyst stability is higher due to the presence of surface defects on MWCNTs and strong metal−support interaction.

Earlier, a Ru/C catalyst can convert glucose to sugar alcohols by a two-step hydrolysis and hydrogenation reaction.[71] Another multifunctional catalyst, MgO/CNT/Pd, is useful in biphasic systems where condensation (metal oxide) and hydrogenation (CNT/Pd) reactions take place on the water−oil interface. In this biphasic system, molecules with a long chain become progressively hydrophobic and migrate from the aqueous to organic phase.[93] MgO/CNT/Pd hybrids are used for the base-catalyzed aldol condensation of furfural with acetone followed by the hydrogenation to form C8−C10 fuel-range molecules (Figure 15).[94]

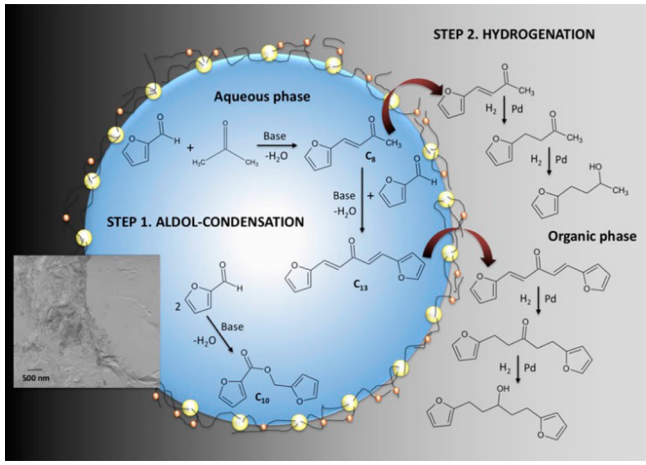

Figure 15. Schematic illustration of the aldol condensation and hydrogenation reactions taking place at the water/oil interface in nanohybrid-stabilized emulsions. Reproduced from ref 94.

Esterification. Interest in biodiesel research has increased over the years due to diminishing petroleum reserves.[95,96] Typically, a triglyceride is esterified with alcohol to produce biodiesel alkyl esters and glycerol (Figure 16). Despite its high volume, fuel is considered a low value product, and the future development of biofuels and biodiesels is dictated by the future development of oil and gas prices. New processes must be developed to transform biomass, preferably from nonfood sources, to fuels in the most economically competitive way.

Sulfonated carbon catalysts derived from glucose are used for the esterification of long chain fatty acids such as oleic acid and stearic acid which can be converted to high grade biodiesel.[97] They are more active than both Nafion NR50 and niobic acid, but their activity is only half that of H_2SO_4. The same carbon material could be used for the transformation of biodiesel from oleic acid at 353 K (with a catalytic activity 70−80% that of sulfuric acid) and the transesterification of triolein at 403 K.[98] Transesterification occurs on the carbon catalyst with

dx.doi.org/10.1021/cs5008393 | ACS Catal. 2014, 4, 3393−3410

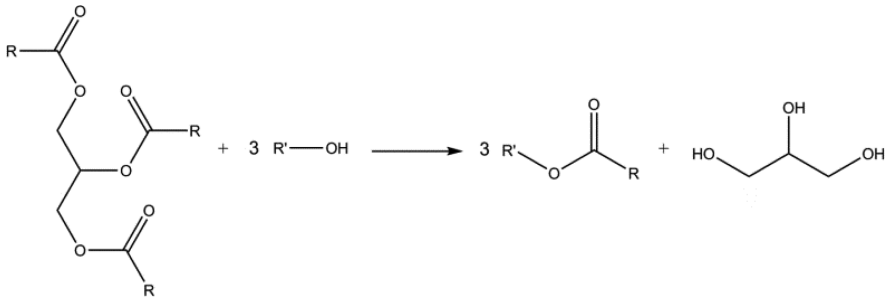

Figure 16. Biodiesel formation.

suppression of free higher fatty acid and monoglyceride formation in the presence of sufficient water. The strong hydrogen bonding interaction between the hydrophilic reactants and the OH groups of the catalyst material promotes reactivity in contrast to solid acids, such as Nafion and Amberlyst with hydrophobic backbones that would repel the reactants. Similarly, nonedible seed oil, *Calophyllum inophyllum*, with free fatty acids of 15% can be converted to biodiesel over carbonized materials with SO_3H groups.[99] The acid-catalyzed reaction of HMF with ethanol using reduced graphene oxide (S-RGO) produces 5-ethoxymethylfurfural, 5-(ethoxymethyl)-furfural diethylacetal, and/or ethyl levulinate.[100] The cooperative effects of the sulfonic acid groups and other types of acid sites (e.g., carboxylic acids), and the enhanced accessibility to the active sites are attributed to the 2D structure. In comparison to carbon black and CNTs, elemental analysis and acid−base titration confirmed that S-RGO did not experience leaching of sulfonic acid groups or suffer deactivation after pretreatment with ethanol in forming sulfonic and carboxylic alkyl esters and ethers.

Esterification is quite complex in aqueous environments due to different equilibria involving water. The decreasing rate of esterification could be due to reverse hydrolysis and a competitive protonation step involving water and the alcohol.[101,102] Sulfonated Starbon materials prepared at 400 °C exhibit an enhanced reactivity for the esterification of succinic acid with ethanol compared to H_2SO_4, β-zeolites, DARCO, and sulfated zirconia. A 5-fold increase in the reaction rate over the homogeneous reaction is attributed to changes in a local water concentration in the catalyst active center, although the mesoporous nature of the Starbon material promotes enhanced molecular diffusion compared to other solids acids.

Hydrodeoxygenation. Hydrodeoxygenation (HDO) reactions convert carbohydrates to unsaturated compounds where the catalyst should favor C−O over C−C bond cleavage, with minimal H_2 consumption. Mo_2C exhibits high selectivity toward C−O/C═O cleavage with negligible C−C bond scission, resulting in the favored formation of propylene over propane starting with C3 oxygenates containing C−O or C═O bonds, including propanol, 2-propanol, and acetone.[103] Mo_2C on activated carbon is highly effective for converting various vegetable oil (olive, soya bean, rapeseed, and maize oil) to diesel-range hydrocarbons in comparison to unsupported Mo_2C, due to available active sites while dispersed on the carbon substrate.[104] Mo_2C on MWCNTs, produced by the carbothermal hydrogen reduction method, exhibits HDO capability on vegetable oil.[105] The Mo_2C catalyst can be formed at lower temperatures on MWCNTs than on activated carbon. Compared to activated carbon and CNT, Mo_2C on CNFs produce no branched hydrocarbons during the HDO of vegetable oils to diesel-range hydrocarbons.[106] A two-step conversion of lignin to monoaromatic compounds of low oxygen involves initial lignin depolymerization in a liquid phase reforming (LPR) reaction to produce a lignin-oil, which is then subject to a second HDO reaction over Mo_2C/CNF catalysts. The two-step LPR−HDO process produces over 25% non-oxygen products including benzene, toluene, and xylenes, which cannot be obtained by direct HDO of lignin.[107] Subsequently, greater conversion and selectivity are achieved using Mo_2C on high surface area ordered mesoporous carbon (OMC); the catalyst is produced by a one-pot synthetic method using a solvent-evaporation-induced self-assembly (EISA) approach.[108]

Tungsten carbide (WC) is another highly selective catalyst for the HDO of propanal and propanol to propene. Decreasing the particle size of the WC catalyst, from ∼100 nm to 3−5 nm of Mo_2C, increases the reaction rate as both catalysts may follow a similar mechanistic pathway to produce propene from propanal as the dominant product.[109] CNFs with high mesoporosity and surface area are used to support WO and WC for highly selective decarboxylation/decarbonylation and HDO of biomass-derived glyceride, respectively.[110]

Bio-oils derived from the pyrolysis of woody biomass is limited by high viscosity, low heating value, incomplete volatility, and thermal instability owing to the presence of oxygenated organic compounds in the biomass feedstock.[111] Thus, HDO reactions are needed to upgrade bio-oils. The HDO pathways of guaiacol are illustrated in Figure 17,

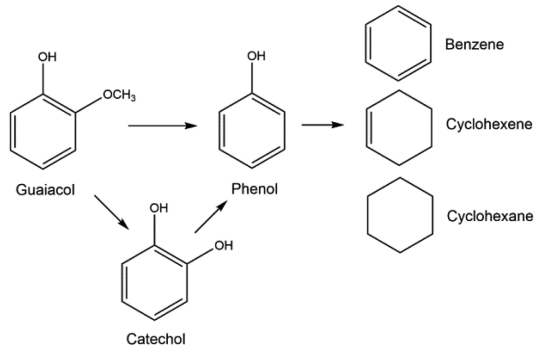

Figure 17. Hydrodeoxygenation of guaiacol.

indicating that guaiacol can undergo demethylation to form catechol and then to phenol, or direct demethoxylation to form phenol. Further deoxygenation of phenol results in benzene, cyclohexene and cyclohexane.[112] Mono- and dimethoxy phenols are predominant in bio-oils; therefore, guaiacol (2-methoxyphenol) often serves as a model compound for HDO studies.[37]

dx.doi.org/10.1021/cs5008393 | ACS Catal. 2014, 4, 3393−3410

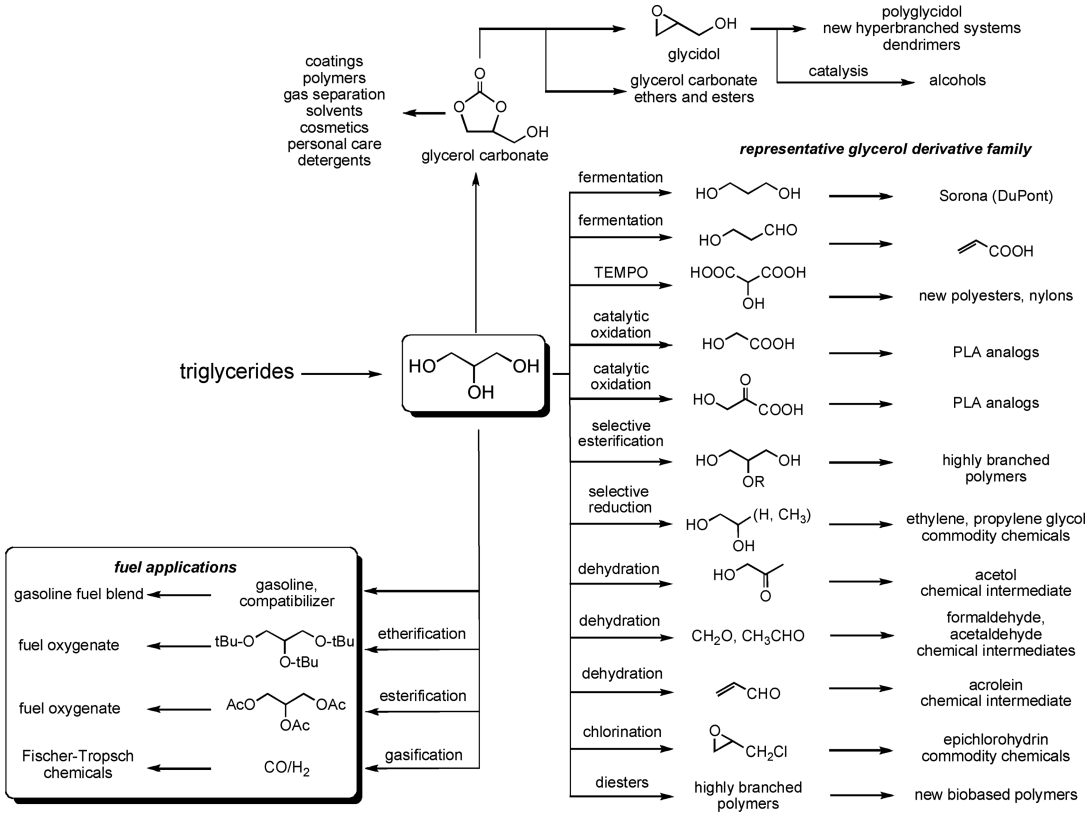

Figure 18. Transformations of glycerol. Reproduced from ref 5.

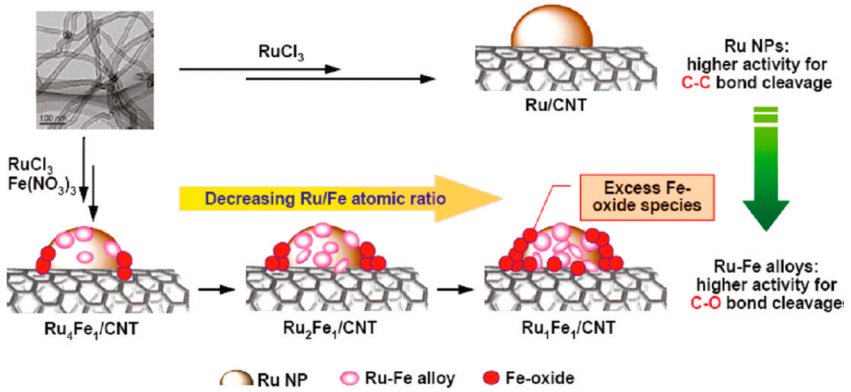

Figure 19. Schematic for preparation of Ru/CNT and RuFe/CNT catalysts and their catalytic behavior in the hydrogenolysis of glycerol. Reproduced from ref 128.

HDO reactions can be conducted over metal sulfides such as sulfided Co(Ni)Mo/γ-Al_2O_3[113,114] supported on alumina[115] and supported noble metal catalysts such as Ru, Rh, and Pd.[116,117] Regeneration with a sulfiding agent contaminates products[118,119] and the acidic nature of the alumina support is prone to substantial coke formation, leading to catalyst deactivation.[120] The alumina support is also unstable in water at processing conditions. Consequently, neutral materials such as Si,[121] Zr,[117,122] and activated carbon,[112,123] have been attempted as catalytic supports. In particular, carbon materials appear to be promising supports for the HDO of bio-oils with negligible coke formation and the direct elimination of the methoxy group of guaiacol to form phenol.

Hydrogenolysis. Glycerol is a major byproduct of biodiesel production; about one pound of glycerol for every gallon of biodiesel produced. An extensive list of potential glycerol transformation products is presented in Figure 18. The biotransformation of crude glycerol produces 1−3-propanediol, citric acid, poly(hydroxyalkanoates), hydrogen, docosahexaenoic acid, lipid, among others. Other routes based on conventional catalytic conversions of glycerol lead to (2,2-dimethyl-1,3-dioxolan-4-yl) methyl acetate as a biodiesel additive,[124] acrolein as an important precursor for producing detergents, acrylic acid ester, and super absorbing polymers.[125] It is notable that it is possible to develop crude glycerol as a fuel for generating electricity from microbial fuel cells.[126]

Metallic NPs on carbon materials play a significant role in catalyzing the transformation of glycerol to value-added chemicals with Ru and Pt NPs on activated carbon showing different selectivities for the hydrogenolysis of glycerol. At neutral pH, Ru is more active than Pt at converting glycerol to glycols, with a preference for ethylene glycol as C−C bond

dx.doi.org/10.1021/cs5008393 | ACS Catal. 2014, 4, 3393−3410

cleavage is postulated to occur over Ru primarily via a metal-catalyzed reaction, whereas Pt favors the formation of propylene glycol. When base is added, the activity of Pt exceeds Ru with ethylene glycol formation through a base-catalyzed retro-aldol reaction. The effect of adding sulfur to Ru/C catalysts suppresses the reaction rate for glycerol conversion due to catalyst poisoning.

A second beneficial effect could be dramatically increasing the selectivity for propylene glycol by promoting an initial crucial dehydration step.[127] A study comparing 3 nm RuFe and Ru NPs on CNT shows that Ru NPs are selective for C−C bond cleavage, whereas RuFe NPs favor the C−O bond cleavage, resulting in higher selectivity for glycol formation from glycerol (Figure 19).

The higher performance of the RuFe/CNT catalyst is attributed to the synergistic effects of the formation of RuFe alloys and the interactions between the RuFe bimetallic NPs and iron oxides on CNT surfaces to improve the catalyst stability.[128] The performance of the activated carbon-supported bimetallic RuFe catalyst was lower than the CNT-supported one under identical conditions. Li and co-workers believe that alignment of lattices along the CNT axis and the curvature of graphite-like planes can bring defect sites and functional groups on the surface, favorable for the electron transfer rates of reaction and the desorption of products to increase catalyst activity. Alternatively, CuRu NPs on CNT display highly disperse Ru NPs on the Cu NP surface. The Ru NPs alone fail to convert glycerol but instead generate active hydrogen that is transferred to the Cu NP surface via hydrogen spillover. The spillover effect increases the hybrid catalyst's activity and selectivity of for the production of 1,2-propanediol compared to Cu NPs alone.[129]

Lactic acid biosynthesis is performed by bacteria with glucose and sucrose as the substrates. Alternatively the conversion of renewable biopolyols to lactic acid usually demands excess hydrogen/oxygen or harsh reaction conditions in strong alkaline medium (220−350 °C). This unfortunately promotes significant side reactions resulting in low carbon selectivity to liquid products, posing significant challenges for the development of sustainable technologies. Figure 20 shows some of the products from the conversion of lactic acid including polylactic acid (PLA), a biodegradable plastic.

Carbon-supported catalysts are able to overcome some of these challenges to produce lactic acid in significant quantities. Highly active Cu-graphene catalysts for the conversion of biopolyols (glycerol, xylitol, and sorbitol) to lactic acid and other diols and linear alcohols was achieved by creating catalytically active [111] facets as the dominant surface by lattice-match engineering.[130] Trace amounts of Pd incorporated into the Cu-graphene system enhance the catalyst stability and result in a tandem synergistic system in which the hydrogen generated in situ from polyols is used for sequential hydrogenolysis of the feedstock itself.

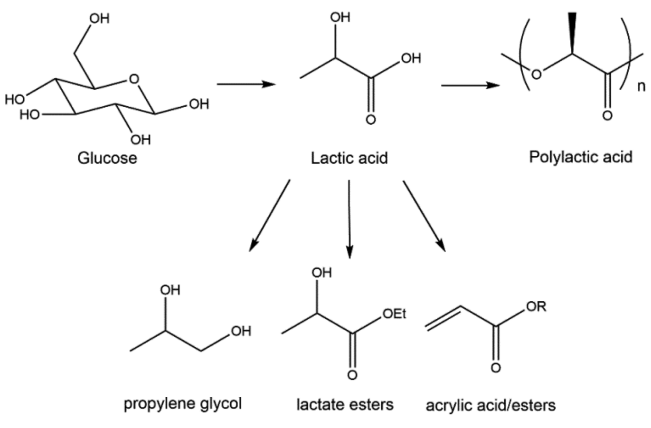

Figure 20. Lactic acid conversion.

Pt/C acts as a multifunctional catalyst for tandem dehydrogenation/hydrogenolysis of polyols in which glycerol, xylitol, mannitol, and sorbitol are converted to lactic acid, and glycols and linear alcohols as coproducts.[131] The reaction at 115−160 °C without hydrogen or oxygen, using Ba^{2+} ion promotes the activity of the Pt/C catalyst by almost 12-fold compared to NaOH, KOH, and $Ca(OH)_2$. Two-thirds of the hydrogen generated in situ via the dehydrogenation of polyols over the Pt/C catalyst is utilized for converting the remaining polyols and intermediates to useful products with the remaining available hydrogen for use elsewhere in the biorefinery setting.

Ru/C outperforms other metal oxides and noble metal NPs for selective hydrogenolysis of biomass-derived xylitol to ethylene glycol and propylene glycol in the presence of $Ca(OH)_2$.[132] Different metals and supports effect dehydrogenation/hydrogenation activities and surface acid-basicity, which consequently influence the xylitol reaction pathways. Initially the dehydrogenation of xylitol to xylose takes place on the metal surfaces, followed by base-catalyzed retro-aldol condensation of xylose to form glycolaldehyde and glyceraldehyde. Glycolaldehyde is then hydrogenated to ethylene glycol, whereas glyceraldehyde is dehydrated and hydrogenated to propylene glycol. The selectivity for the two glycols depends on the relative rates between the hydrogenation of the aldehyde intermediates and their competitive reactions with the bases.

The aqueous phase reforming of xylitol is studied using five Pt/C catalysts with varying Pt cluster sizes and surface acidity.[133] TOF linearly increases with increasing average Pt cluster size. Catalysts with higher surface acidity favor higher rates of hydrocarbon production, but those with lower acidities favor the hydrogen formation. Xylitol can also be converted into ethylene glycol and propylene glycol using the Ni/C catalyst in the presence of CeO_2 and $Ca(OH)_2$.[134] Ni/C exhibits a higher activity for this reaction as compared to Ru/C. In addition, it is possible to decrease the amount of base needed by supporting Ni on the CeO_2/C and CaO/C hybrids.

Oxidation. The selective oxidation of HMF to 5-hydroxymethyl-2-furancarboxylic acid (HFCA), and 2,5-furandicarboxylic acid (FDCA), is widely studied as FDCA is a highly sought intermediate to replace fossil-fuel derived terephthalic acid in aromatic polyesters.[135] PVP-protected Au and its alloys are supported on activated carbon, CNF, CNTs, and graphite.[136] The FDCA formation is highly favored for Au on activated carbon, perhaps due to the smaller Au particle size of 2.9 nm. By alloying Pd to Au to form Au_8−Pd_2, the catalyst reuse is greatly enhanced as the catalyst deactivation by adsorbed intermediates is circumvented compared to Au alone. Most recently, an Au−Pd alloy catalyst supported on CNTs promotes the aerobic oxidation of HMF to FDCA in water without any bases.[137] CNTs containing more carbonyl/quinone and less carboxyl groups favor the FDCA formation by enhancing the adsorption of the reactant and reaction intermediates.

The oxidation of glycerol to glyceric acid,[138] and cellobiose to gluconic acid[139] is facilitated by noble metals such as Pd, Pt,

dx.doi.org/10.1021/cs5008393 | ACS Catal. 2014, 4, 3393−3410

Au, and their alloys (PdAu, PtAu). Carbon is selected as a support in such studies due to its stability in both acidic and basic media. Of also interest is the one-pot conversion of glycerol to lactic acid using monometallic Au and Pt as well as bimetallic (Au−Pt) catalysts supported on nanocrystalline CeO_2 (n-CeO_2) in aqueous solution in the presence of a base and oxygen.[140] The bimetallic system shows excellent activity (TOF = 1170 h^{-1} for a batch time of 20 min) with a high selectivity (80%) to lactic acid at 99% glycerol conversion (373 K, NaOH to glycerol molar ratio of 4:1 and 5 bar oxygen). The Au−Pt/n-CeO_2 catalyst can be recycled five times in a batch setup without a significant decrease in activity and lactic acid selectivity.

BIOCATALYSIS ON CARBON SUPPORT MATERIALS

Immobilized enzymes are increasingly used as catalysts for the preparation of fine and specialty chemicals because they facilitate the product recovery and the biocatalyst reuse. Many supports have been studied extensively for enzyme immobilization, including polymers and resins, silica and silica−alumina composites, and carbonaceous materials in the form of powders, beads, or chips. Such operating systems are often severely diffusion limited, leading to a considerable fraction of unused enzymatic activity. Other classical problems inherent to bioprocessing using microorganisms include low efficiencies, narrow reaction conditions, contamination, and limited scale of production compared to chemical processing.[141,142]

Ceramic honeycomb monoliths can be functionalized with different carbon coatings such as sucrose carbonization, polymer carbonization, and growth of CNFs. In brief, sucrose-based carbon carriers can be prepared by dipping monoliths in a 65% sucrose solution in water, followed by air-drying at 393 K for 4 h and carbonization for 2 h under H_2 at 823 K.[143] Similarly, polyfurfuryl alcohol (PFA)-based carbon coatings are prepared by coating monoliths with freshly prepared PFA solution followed by air drying at 353 K and carbonization at 823 K under Ar for 2 h.[144]

Laccase immobilized on different carbon materials[145] is feasible for the delignification of lignocellulose. Graphene oxides are most efficient to immobilize the maximum amount of laccase and retain high activity of the immobilized enzyme. The solution pH plays a significant role in laccase immobilization and activity; deviations from neutral pH result in lower enzyme loading and activity. Reduced graphene might not be useful due to its hydrophobic nature to form aggregates in the aqueous solution.

Glucoamylase (GA) was immobilized by adsorption on different carbon supports including Sibunit (porous carbon−carbon composite materials combining the elements of graphite and active coals), bulk catalytic filamentous carbon, and activated carbon for the hydrolysis of starch dextrin.[146] The thermal stability of immobilized GA improves by 2−3 orders of magnitude in comparison with the soluble enzyme, in which the enzyme on Sibunit exhibits the best performance. The dextrin hydrolysis rate using the GA/Sibunit biocatalyst in an immersed vortex reactor was increased by a factor of 1.2−1.5 compared to the packed-bed reactor.

CNFs are grown on an alumina or silica washcoat layer with Ni deposited on the support at 353 K from a 1 M aqueous urea solution.[147] After reduction for 1 h at 973 K, CNFs are grown under propene or methane in N_2.[148] Such resulting carriers have tunable surface area, pore size distribution and hydrophobicity and serve as excellent supports for biocatalysts. In a similar example, branching CNTs can enhance the activity of carbonized cellulosic fibers in combination with glycerol dehydrogenase for the biotransformation of glycerol to dihydroxyacetone.[149] Alternatively, magnetic graphene-based catalysts for cellulase immobilization are produced by the assembly of oppositely charged quenched polyelectrolytes and magnetic NPs on graphene; followed by covalent immobilization of cellulase through annealed polyelectrolyte brushes and zero-length spacer molecules. The activity of immobilized cellulase evaluated against carboxymethylcellulose and microcrystalline cellulose shows a 1.5-fold improvement in activity for enzymes immobilized on annealed polyelectrolyte brushes compared to immobilized enzymes without the brushes.[150]

From the context of biomass transformation, the production of HMF from fructose can be obtained by the isomerization of glucose.[151] In this case, glucose isomerase, a well-known and commercially available enzyme, can be easily immobilized on the above carbon coated carriers to perform the transformation. Most recently, glucose isomerase enzyme was immobilized on a base (NH_2) functionalized mesoporous silica (aminopropyl-FMS). The combination of this catalyst with a Brønsted acid (SO_3H) functionalized mesoporous silica (propylsulfonic acid-FMS) allowed for the one-pot conversion of glucose to HMF directly in a monophasic solvent system of THF and H_2O (4:1 v/v) with 61% and 30% yield of fructose and HMF, respectively over 24 h at 363 K.[152] Other useful enzymes for biomass transformation includes cellulosic enzymes (cellulose hydrolysis), ligninase (breakdown of lignin), lipase (hydrolysis of fats and lipids), xylanase (hemicellulose hydrolysis), and so forth.

CRITICAL ANALYSIS

Potentials of Biorefinery. Biorefinery processing relies on chemical (gasification, pyrolysis, or direct liquefaction), enzymatic, and microbial transformations to convert biomass into a wide range of specialty chemicals. For biorefinery applications to be "green", the process should be selective, energetically efficient, high yielding, and environmentally benign. Integrated biorefinery technologies require significant investments in research, development, deployment, and cost reduction to be competitive with chemical processing of fossil oils. There are always high risks associated with new technology deployment. Many technologies in the early stages of development still require ongoing financial and social support, particularly for the production of advanced fuels. Environmental impact is always a key issue because feedstocks and conversion processes used in one specific biorefinery might have unique, negative impacts on the environment.

The combination of enzymes/biomolecules with carbon-based catalysts/supports for more efficient conversion of biomass by cascade catalysis is an important approach and deserves more attention. Bioconversion of phenol and some selected acids such as lactic, succinic, levulinic, and butyric acids has become more competitive owing to significant improvements in microbial conversion and product separation technology. Lastly, the effect of residual impurities of feedstocks on the activity and/or the selectivity of catalysts must be fully addressed. Detailed information on catalyst deactivation and regeneration using "real-world" biomass feedstocks instead of "off-the-shelf" molecules needs to be established.

Potentials of Carbon Materials. To date, carbon materials only have a modest position in industrial catalytic processes, and their full potential has not been exploited. During the past decade, emerging carbon nanomaterials have received signifi-

dx.doi.org/10.1021/cs5008393 | ACS Catal. 2014, 4, 3393−3410

cant attention, but their applications in catalysis are still very limited. In addition to their high cost and large-scale unavailability, some fundamental issues related to the surface area, surface chemistry, and structure must be addressed to pave the way for their large scale applications. In general, carbon supports are attractive for heterogeneous catalysis because the carbon surface is more inert than in typical oxide supports. Carbon materials offer unparalleled flexibility in tailoring their properties (physical and chemical) to specific needs, thus illustrating the remarkably wide range of potential applications. They are also excellent hosts for metallic NPs, where hybrid materials serve as a multifunctional catalyst in many biomass transformation reactions. As mentioned earlier, many factors to improve catalyst activity can be linked to both the physical properties of carbon (high surface area, porous structure) and the chemical properties (oxygenated groups, sulfonic acid groups).

Carbon Materials as Solid Acids. Carbon materials can be made active for acid catalytic reactions by sulfonation, a fairly simple and straightforward procedure. In particular, carbon materials activated by a chemical process are better suited for the synthesis of carbon-based solid acid catalysts.[49] However, the catalytic activity and the selectivity of solid catalysts to the desired products are quite low, compared with liquid acid catalysts, for instance, in cellulose hydrolysis.[63,67] Such results are not totally unexpected because both lignocellulosic biomass and solid catalysts are insoluble in water. The H^+ ions from solid Brønsted acids or the active sites from solid Lewis acids are difficult to access by reactants, resulting in a low reaction activity. Unreacted cellulose from sticky residues and various insoluble products might be adsorbed onto the solid acid catalysts to deactivate their activity.[63] Ionic liquids can be used to dissolve microcrystalline cellulose along with solid acids (e.g., Amberlyst catalysts in 1-butyl-3-methylimidazolium chloride) to break down cellulose into oligomers (10 glucose units) due partly to the easy release of H^+ ions into the solvent.[153] To date, ionic liquids are still exorbitant in price for industrial applications, besides their questionable large-scale availability. Nevertheless, ionic liquids and supercritical fluids may provide higher catalytic efficiency than conventional media. Together with activation treatments (e.g., ultrasounds or microwaves), such fluids might receive more attention in bioprocessing, and considerable investigations are required to better characterize and evaluate the performance of metal catalysts in such reaction media.

The reusability of sulfonated carbon catalysts have been put to question by several reports of leaching of sulfonated groups.[154] Methods to measure the decrease in acid content may include elemental analysis for sulfur, acid−base back-titration, and X-ray photoelectron spectroscopy (XPS). Direct sulfonation of activated carbon leads to the formation of weak (phenolic groups), medium (lactonic groups), and strong acid sites (carboxylic and/or sulfuric groups). A substantial loss in total acidic sites has been noticed when these materials are subjected to treatment with hot water (150 to 225 °C) over 24 h.[155] The leaching of sulfonated species may homogeneously catalyze biomass reactions at these hydrothermal conditions (for example, the hydrolysis of xylose to furfural) in combination with heterogeneous catalysis by acidic carbon materials. The loss of unstable acidic groups should reduce the activity of the catalyst, dampening the prospects of recovering and reusing the carbon material as a catalyst. However, an aging step in hot liquid water could be used to remove the unstable groups prior to a catalytic process. Consequently, a significant fraction of the strong acidic sites remains stable on the carbon surface after hydrothermal treatment.[69,156] Such pretreated materials would be preferable in terms of reusability and accurate determination of reaction mechanism/kinetics.

Metal-Doped Carbon Catalysts. Metal-doped carbon is easily prepared by following three main strategies: by addition of the metal precursor to the initial mixture, by ion-exchange or by deposition of the metal precursor on the organic or the carbon material. Unsupported metal NP catalysts are likely to agglomerate in solution, and their recovery is very complicated. However, when bound to carbon supports, the NPs are likely to remain stable and well-dispersed on the carbon surface with opportunities for their facilitated recovery and reuse. Support materials with well-defined pore sizes and high surface area can be fabricated into different form factors from inexpensive biomass material. They are easily functionalized with oxygen-bearing surface groups to increase the contact between carbon support and a noble metal precursor for more uniform particle distribution. In functionalizing the support material, one must consider the ramifications of functional group leaching, the hydrogen spillover effect, and the attraction of reactants toward the catalyst surface with changes in hydrophilicity.

Two metals, Ru and Au, play an important role in biomass conversion; the former is for hydrogenation, hydrolysis/hydrogenation, and hydrogenolysis/dehydroxylation reactions, whereas the latter is for oxidation reactions. Compared to conventional Ni catalysts for carbohydrate hydrogenation, Ru catalysts also exhibit a significantly higher specific or intrinsic hydrogenation activity. They also have a higher resistance to sintering and leaching in acidic and chelating aqueous solutions. The dissociation of water molecules on the Ru surface might attribute to the high hydrogenation activity, but more studies are required to decipher the reasons why Ru catalysts are more active and selective for reduction of aldehydes, ketones, and carboxylic acids than other Pt-group metals. The selective oxidation of alcohols to aldehydes in aqueous solutions using supported Au NPs has been a remarkable discovery albeit the oxidation mechanism of alcohols by Au catalysts remains unknown. One plausible explanation is their capability to activate dioxygen at the solid−liquid interface in the presence of water to double the adsorption energy.[157] However, Au NPs can lose their activity easily via coalescence or Ostwald ripening processes, and regeneration of Au NPs should be established for practical applications.

Bimetallic or multimetallic catalysts should be designed to improve catalytic activity, selectivity and stability and allow for one-pot conversion. Bimetallic Pd_xAu_y/C catalysts also exhibit a significant activity for selective hydrogenation of HMF toward DMF compared to monometallic Pd/C and Au/C catalysts.[158] Pd−Ag bimetallic catalysts supported on texture-tailored carbon xerogels have been tested for hydrodechlorination of 1,2 dichloroethane into ethylene.[159] Pure Pd catalyst is active, but deactivation occurs quickly with low ethylene selectivity. The ethylene selectivity increases with increasing Ag content of the alloy. Carbon xerogels as supports for Pt and Pt−Sn bimetallic catalysts have also been attempted in the hydrogenation of cinnamaldehyde.[160] A 96% conversion with 68% selectivity to cinnamyl alcohol after 8 h at 60 °C and 5 bar can be achieved in a mixed solvent.

Molybdenum and tungsten-oxide-doped monolithic carbon aerogels have been investigated in the isomerization reaction of 1-butene.[161] In particular, the latter is more active than those

dx.doi.org/10.1021/cs5008393 | ACS Catal. 2014, 4, 3393−3410

with chromium or molybdenum oxide. Pt catalysts supported on carbon aerogels have been used in the toluene combustion reaction.[162] Complete toluene oxidation is reached in the range between 160 and 230 °C, compared to 200 °C reported for some Pt/Al_2O_3 catalysts.[163] To date, metal-doped carbon aerogels have been tested in only a few reactions. It is anticipated that the use of carbon aerogels for catalytic applications will increase for the future transformation of chemicals derived from biomass to higher value products. Carbon monoliths can be fabricated from the pyrolysis of a resorcinol−formaldehyde copolymer on silica particle templates with iron serving as the catalyst for localized carbonization. The resulting polymer can be doped with a metallic salt, in turn forming encapsulated metallic NPs during the course of carbonization.[164] Such resulting carbon monoliths with metallic NPs could be excellent catalysts in biomass transformation.

Base metals on carbon supports is a desirable future endeavor, although there is a high risk of metal leaching in solutions due to the chelating properties of carbohydrates and derivatives. The excellent properties of graphene stem mainly from the planar direction compared to the axial direction of its CNTs counterpart. Thus, the combined one-dimensional CNTs and two-dimensional graphene pair could be an excellent catalyst support. Pt or other metallic NPs can be loaded over this hybrid support by different procedures including chemical reduction. Indeed, this concept was attempted for in situ preparation of a hybrid composite material using graphene and MWCNTs by solar exfoliation of a graphene oxide−MWCNT composite.[165] MWCNTs effectively prevent the restacking of graphene to allow a uniform distribution of Pt NPs over the graphene and MWCNTs by chemical reduction. CNTs and graphene-based nanomaterials are promising metal-free electrocatalysts besides their excellent catalyst support properties.

Heteroatoms on the Carbon Network. The role of other heteroatoms on the surface of the carbon catalyst support has not been addressed adequately. In particular, nitrogen can be incorporated in carbon materials by treating the carbon with ammonia at 400 to 800 °C.[166] Indeed, prenitrided carbons provide Mo catalysts with enhanced activity,[167] and a similar effect has been observed for Fe/C and Ru/C catalysts.[168] As well, graphene can be doped with nitrogen and other doping elements such as boron,[169] sulfur,[170] and selenium in fuel cell applications. Nitrogen-doped graphene exhibits much better electrocatalytic activity than a Pt-based oxygen reduction reaction (ORR) catalyst.[171] I-doped graphene (IG) can be prepared by annealing graphite oxide and iodine in Ar with the iodine bonding states identified as triiodide (I^{3-}) and pentaiodide (I^{5-}). The former structure plays a crucial role in the enhancement of ORR activity.[172] Co-doping of carbon materials with two elements, one with higher electronegativety, N (χ = 3.04), and the other with lower electronegativity, B (χ = 2.04), than that of C (χ = 2.55), could create a unique electronic structure with a synergistic coupling effect between such two heteroatoms to render such dual-doped G catalysts much more active than singly doped graphene catalysts. Of attention is a two-step strategy to synthesize B- and N-co-doped graphene.[173] In this procedure, N is first incorporated by annealing with NH_3 at 500 °C followed by the incorporation of B by pyrolysis of nitrogen doped graphene with H_3BO_3 at 900 °C. Doubtlessly, such doped carbon materials will soon find their potential catalytic applications in biomass transformation.

Reactor Design. Although the reactor design in catalytic transformation is beyond the scope of this review, it deserves a brief description here. In the production of fine chemicals, a stirred tank reactor (STR) is mostly applied to control the reaction time, catalyst loading, heating, cooling, and mixing. STR, however, exhibits several shortcomings such as the catalyst separation from the reaction mixture, attrition and agglomeration of the catalyst particles, and safety in case of a runaway reaction. A novel concept is to use a structured reactor embedded with a heterogeneous catalyst in the form of a well-defined geometry. A reactor type that receives increasing attention is the monolithic reactor, consisting of small parallel channels.[174−177] The catalyst can be applied onto the walls of the monolith channels which can be round, square, or triangular, and the material for the walls can be either a metal or a ceramic. However, the maximum catalyst loading in the monolithic stirrer reactor is approximately 4 wt % compared to 10 wt %, which can easily be reached in the slurry reactors. Alternatively, the use of biobased materials like carbonization furfuryl alcohol-based polymers[144] to augment a microporous carbon-coating monolithic support could improve the surface properties for enhanced catalytic activity.

■ CONCLUDING REMARKS

As one of the current topics in chemistry, the catalytic conversion of lignocellulosic biomass into valuable chemicals and products involves many technical challenges and opportunities. Considerable attention has focused on the chemocatalytic conversion of cellulose over hemicellulose and lignin. Apparently, the most achievable and economical way is to convert lignocellulosic biomass directly, rather than pure cellulose, hemicellulose, or lignin. In this context, such technology remains in its infancy and requires continual technological innovations and breakthroughs. As long as fossil crude oils are still available in large quantities, the production of fuels and chemicals from biomass is still not cost competitive.

Emerging porous carbon materials are leading candidates for carbon-supported catalysts and carbon catalysts in biomass transformation applications. Both physical (surface area and porosity) and chemical properties (functional groups, immobilized metal NPs, and enzymes) of carbon materials must be taken into account for the design of an effective catalyst with high activity and selectivity. However, there are still several pending issues that require considerable research and development: (i) in-depth insights into the heterogeneously catalytic conversion of lignocellulosic biomass; and (ii) strategic use of multifunctional catalysts for processing biomass as a whole, not its individual components such as cellulose, hemicellulose, and lignin.

■ AUTHOR INFORMATION

Corresponding Author

*E-mail: j.luong@ucc.ie.

Notes

The authors declare no competing financial interest.

■ REFERENCES

(1) Berger, M. W. Biorefinery concept shows a way out of a world dominated by petrochemicals. http://www.nanowerk.com/spotlight/spotid=16508.php#ixzz32GqsvxDi (accessed May 22, 2014).

(2) Diercks, R.; Arndt, J. D.; Freyer, S.; Geier, R.; Machhammer, O.; Schwartze, J.; Volland, M. *Chem. Eng. Technol.* **2008**, *31*, 631−637.

(3) Langholtz, M.; Downing, M.; Graham, R.; Baker, F.; Compere, A.; Griffith, W.; Boeman, R.; Keller, M. *SAE Int. J. Mater. Manuf.* **2014**, *7*, 115−121.

(4) Stewart, D. *Ind. Crops Prod.* **2008**, *27*, 202−207.
(5) Bozell, J. J.; Petersen, G. R. *Green Chem.* **2010**, *12*, 539−554.
(6) Dauenhauer, P. J.; Huber, G. W. *Green Chem.* **2014**, *16*, 382−383.
(7) Dapsens, P. Y.; Mondelli, C.; Pérez-Ramírez, J. *ACS Catal.* **2012**, *2*, 1487−1499.
(8) Matthiesen, J.; Hoff, T.; Liu, C.; Pueschel, C.; Rao, R.; Tessonnier, J.-P. *Chin. J. Catal.* **2014**, *35*, 842−855.
(9) Rodriguez-Reinoso, F. *Carbon* **1998**, *36*, 159−175.
(10) Falcao, E. H. L.; Wudl, F. *J. Chem. Technol. Biotechnol.* **2007**, *82*, 524−531.
(11) Titirici, M.-M.; Antonietti, M. *Chem. Soc. Rev.* **2010**, *39*, 103−116.
(12) Ajayan, P. M. *Chem. Rev.* **1999**, *99*, 1787−1800.
(13) Geim, A. K.; Novoselov, K. S. *Nat. Mater.* **2007**, *6*, 183−191.
(14) Zhang, K.; Yue, Q.; Chen, G.; Zhai, Y.; Wang, L.; Wang, H.; Zhao, J.; Liu, J.; Jia, J.; Li, H. *J. Phys. Chem. C* **2011**, *115*, 379−389.
(15) Nam, K.-W.; Song, J.; Oh, K.-H.; Choo, M.-J.; Park, H.; Park, J.-K.; Choi, J. W. *Carbon* **2012**, *50*, 3739−3747.
(16) Vinayan, B. P.; Ramaprabhu, S. *Nanoscale* **2013**, *5*, 5109−5118.
(17) Shao, Y.; Zhang, S.; Wang, C.; Nie, Z.; Liu, J.; Wang, Y.; Lin, Y. *J. Power Sources* **2010**, *195*, 4600−4605.
(18) Kong, X.-K.; Chen, C.-L.; Chen, Q.-W. *Chem. Soc. Rev.* **2014**, *43*, 2841−2857.
(19) Jafri, R. I.; Rajalakshmi, N.; Ramaprabhu, S. *J. Mater. Chem.* **2010**, *20*, 7114−7117.
(20) Budarin, V.; Clark, J. H.; Hardy, J. J. E.; Luque, R.; Milkowski, K.; Tavener, S. J.; Wilson, A. J. *Angew. Chem., Int. Ed.* **2006**, *45*, 3782−3786.
(21) Shuttleworth, P. S.; Budarin, V.; White, R. J.; Gun'ko, V. M.; Luque, R.; Clark, J. H. *Chem.—Eur. J.* **2013**, *19*, 9351−9357.
(22) White, R. J.; Budarin, V. L.; Clark, J. H. *ChemSusChem* **2008**, *1*, 408−411.
(23) White, R. J.; Budarin, V.; Luque, R.; Clark, J. H.; Macquarrie, D. J. *Chem. Soc. Rev.* **2009**, *38*, 3401−3418.
(24) Liang, Y. Y.; Li, Y. G.; Wang, H. L.; Dai, H. J. *J. Am. Chem. Soc.* **2013**, *135*, 2013−2036.
(25) Wang, X. R.; Tabakman, S. M.; Dai, H. J. *J. Am. Chem. Soc.* **2008**, *130*, 8152−8153.
(26) Moreno-Castilla, C.; Maldonado-Hodar, F. J. *Carbon* **2005**, *43*, 455−465.
(27) Sevilla, M.; Fuertes, A. B. *Carbon* **2013**, *56*, 155−166.
(28) Svec, F. *J. Chromatogr. A* **2010**, *1217*, 902−924.
(29) Lu, A.-H.; Schüth, F. *Adv. Mater.* **2006**, *18*, 1793−1805.
(30) Knox, J. H.; Gilbert, M. T. (Shandon Southern Products Limited). Depositing polymerizable material onto porous substrate, pyrolysis, graphitization. U.S. Patent 4,263,268, April 21, 1981.
(31) Minakuchi, H.; Nakanishi, K.; Soga, N.; Ishizuka, N.; Tanaka, N. *J. Chromatogr. A* **1997**, *762*, 135−146.
(32) Meng, Y.; Gu, D.; Zhang, F. Q.; Shi, Y. F.; Yang, H. F.; Li, Z.; Yu, C. Z.; Tu, B.; Zhao, D. Y. *Angew. Chem., Int. Ed.* **2005**, *44*, 7053−7059.
(33) Huang, Y.; Cai, H.; Feng, D.; Gu, D.; Deng, Y.; Tu, B.; Wang, H.; Webley, P. A.; Zhao, D. *Chem. Commun.* **2008**, *23*, 2641−2643.
(34) Wang, Y.; Tao, S.; An, Y. *Microporous Mesoporous Mater.* **2012**, *163*, 249−258.
(35) Xu, S.; Li, J.; Qiao, G.; Wang, H.; Lu, T. *Carbon* **2009**, *47*, 2103−2111.
(36) Pierre, A. C.; Pajonk, G. M. *Chem. Rev.* **2002**, *102*, 4243−4266.
(37) Elliott, D. C.; Hart, T. R. *Energy Fuels* **2008**, *23*, 631−637.
(38) Sharma, S.; Pollet, B. G. *J. Power Sources* **2012**, *208*, 96−119.
(39) Machek, V.; Hanika, J.; Sporka, K.; Ruzicka, V.; Kunz, J. *Collect. Czech. Chem. Commun.* **1981**, *46*, 3270−3277.
(40) Stevenson, S. A.; Dumesic, J. A.; Baker, R. T. K.; Ruckenstein, E. *Metal−Support Interactions in Catalysis, Sintering, and Redispersion*; Van Nostrand Reinhold: New York, 1987.
(41) Zhao, H.; Kwak, J. H.; Wang, Y.; Franz, J. A.; White, J. M.; Holladay, J. E. *Energy Fuels* **2006**, *20*, 807−811.
(42) Schacht, C.; Zetzl, C.; Brunner, G. *J. Supercrit. Fluids* **2008**, *46*, 299−321.
(43) Rogalinski, T.; Liu, K.; Albrecht, T.; Brunner, G. *J. Supercrit. Fluids* **2008**, *46*, 335−341.
(44) Nakajima, K.; Hara, M. *ACS Catal.* **2012**, *2*, 1296−1304.
(45) Misono, M. *C. R. Acad. Sci., Ser. IIc: Chim.* **2000**, *3*, 471−475.
(46) Clark, J. H. *Acc. Chem. Res.* **2002**, *35*, 791−797.
(47) Zhou, C. H. *Appl. Clay Sci.* **2011**, *53*, 87−96.
(48) Okuhara, T. *Chem. Rev.* **2002**, *102*, 3641−3665.
(49) Hara, M.; Yoshida, T.; Takagaki, A.; Takata, T.; Kondo, J. N.; Hayashi, S.; Domen, K. *Angew. Chem. Int. Ed.* **2004**, *43*, 2955−2958.
(50) Toda, M.; Takagaki, A.; Okamura, M.; Kondo, J. N.; Hayashi, S.; Domen, K.; Hara, M. *Nature* **2005**, *438*, 178.
(51) Okamura, M.; Takagaki, A.; Toda, M.; Kondo, J. N.; Tatsumi, T.; Domen, K.; Hara, M.; Hayashi, S. *Chem. Mater.* **2006**, *18*, 3039−3045.
(52) Kitano, M.; Arai, K.; Kodama, A.; Kousaka, T.; Nakajima, K.; Hayashi, S.; Hara, M. *Catal. Lett.* **2009**, *131*, 242−249.
(53) Sousa-Aguiar, E. F.; Appel, L. G.; Zonetti, P. C.; do Couto Fraga, A.; Bicudo, A. A.; Fonseca, I. *Catal. Today* **2014**, *234*, 13−23.
(54) Moreno-Castilla, C.; Carrasco-Marin, F.; Maldonado-Hodar, F. J.; Rivera-Utrilla, J. *Carbon* **1998**, *36*, 145−151.
(55) Lv, Y.; Zhang, F.; Dou, Y.; Zhai, Y.; Wang, J.; Liu, H.; Xia, Y.; Tu, B.; Zhao, D. *J. Mater. Chem.* **2012**, *22*, 93−99.
(56) Jansen, R. J. J.; van Bekkum, H. *Carbon* **1995**, *33*, 1021−1027.
(57) Liang, C.; Li, Z.; Dai, S. *Angew. Chem., Int. Ed.* **2008**, *47*, 3696−3717.
(58) Zhang, W.; Tao, H.; Zhang, B.; Ren, J.; Lu, G.; Wang, Y. *Carbon* **2011**, *49*, 1811−1820.
(59) Suganuma, S.; Nakajima, K.; Kitano, M.; Yamaguchi, D.; Kato, H.; Hayashi, S.; Hara, M. *J. Am. Chem. Soc.* **2008**, *130*, 12787−12793.
(60) Kitano, M.; Yamaguchi, D.; Suganuma, S.; Nakajima, K.; Kato, H.; Hayashi, S.; Hara, M. *Langmuir* **2009**, *25*, 5068−5075.
(61) Suganuma, S.; Nakajima, K.; Kitano, M.; Yamaguchi, D.; Kato, H.; Hayashi, S.; Hara, M. *Solid State Sci.* **2010**, *12*, 1029−1034.
(62) Yamaguchi, D.; Kitano, M.; Suganuma, S.; Nakajima, K.; Kato, H.; Hara, M. *J. Phys. Chem. C* **2009**, *113*, 3181−3188.
(63) Onda, A.; Ochi, T.; Yanagisawa, K. *Green Chem.* **2008**, *10*, 1033−1037.
(64) Yamaguchi, D.; Hara, M. *Solid State Sci.* **2010**, *12*, 1018−1023.
(65) Suganuma, S.; Nakajima, K.; Kitano, M.; Hayashi, S.; Hara, M. *ChemSusChem* **2012**, *5*, 1841−1846.
(66) Dora, S.; Bhaskar, T.; Singh, R.; Naik, D. V.; Adhikari, D. K. *Bioresour. Technol.* **2012**, *120*, 318−321.
(67) Pang, J. F.; Wang, A. Q.; Zheng, M. Y.; Zhang, T. *Chem. Commun.* **2010**, *46*, 6935−6937.
(68) Chung, P.-W.; Charmot, A.; Gazit, O. M.; Katz, A. *Langmuir* **2012**, *28*, 15222−15232.
(69) Chung, P.-W.; Charmot, A.; Olatunji-Ojo, O. A.; Durkin, K. A.; Katz, A. *ACS Catal.* **2014**, *4*, 302−310.
(70) Gazit, O. M.; Katz, A. *J. Am. Chem. Soc.* **2013**, *135*, 4398−4402.
(71) Komanoya, T.; Kobayashi, H.; Hara, K.; Chun, W.-J.; Fukuoka, A. *ChemCatChem* **2014**, *6*, 230−236.
(72) Hilgert, J.; Meine, N.; Rinaldi, R.; Schüth, F. *Energy Environ. Sci.* **2013**, *6*, 92−96.
(73) Deng, W. P.; Tan, X. S.; Fang, W. H.; Zhang, Q. H.; Wang, Y. *Catal. Lett.* **2009**, *133*, 167−174.
(74) Zhang, Y.; Wang, A.; Zhang, T. *Chem. Commun.* **2010**, *46*, 862−864.
(75) Park, D. S.; Yun, D.; Kim, T. Y.; Baek, J.; Yun, Y. S.; Yi, J. *ChemSusChem* **2013**, *6*, 2281−2289.
(76) Hu, L.; Zhao, G.; Hao, W.; Tang, X.; Sun, Y.; Lin, L.; Liu, S. *RSC Adv.* **2012**, *2*, 11184−11206.
(77) van Putten, R.-J.; van der Waal, J. C.; de Jong, E.; Rasrendra, C. B.; Heeres, H. J.; de Vries, J. G. *Chem. Rev.* **2013**, *113*, 1499−1597.
(78) Teong, S. P.; Yi, G.; Zhang, Y. *Green Chem.* **2014**, *16*, 2015−2026.
(79) Wang, T.; Nolte, M. W.; Shanks, B. H. *Green Chem.* **2014**, *16*, 548−572.
(80) Lam, E.; Chong, J. H.; Majid, E.; Liu, Y.; Hrapovic, S.; Leung, A. C. W.; Luong, J. H. T. *Carbon* **2012**, *50*, 1033−1043.

(81) Russo, P. A.; Lima, S.; Rebuttini, V.; Pillinger, M.; Willinger, M.-G.; Pinna, N.; Valente, A. A. *RSC Adv.* **2013**, *3*, 2595−2603.
(82) Qi, X. H.; Guo, H. X.; Li, L. Y.; Smith, R. L. *ChemSusChem* **2012**, *5*, 2215−2220.
(83) Liu, R. L.; Chen, J. Z.; Huang, X.; Chen, L. M.; Ma, L. L.; Li, X. J. *Green Chem.* **2013**, *15*, 2895−2903.
(84) Daengprasert, W.; Boonnoun, P.; Laosiripojana, N.; Goto, M.; Shotipruk, A. *Ind. Eng. Chem. Res.* **2011**, *50*, 7903−7910.
(85) Mazzotta, M. G.; Gupta, D.; Saha, B.; Patra, A. K.; Bhaumik, A.; Abu-Omar, M. M. *ChemSusChem* **2014**, *7*, 2342−2350.
(86) Filikov, A. V.; Myasoedov, N. F. *J. Phys. Chem.* **1986**, *90*, 4915−4916.
(87) Keren, E.; Soffer, A. *J. Catal.* **1977**, *50*, 43−55.
(88) Wang, D.; Niu, W.; Tan, M.; Wu, M.; Zheng, X.; Li, Y.; Tsubaki, N. *ChemSusChem* **2014**, *7*, 1398−1406.
(89) Suh, D. H.; Park, T.-Jin; Ihm, S.-K. *Carbon* **1993**, *31*, 427−435.
(90) Luque, R.; Clark, J. H.; Yoshida, K.; Gai, P. L. *Chem. Commun.* **2009**, *35*, 5305−5307.
(91) Härkönen, M.; Nuojua, P. *Kemia-Kemi* **1979**, *6*, 445−447.
(92) Liang, X.; Jiang, C. *J. Nanopart. Res.* **2013**, *15*, 1890.
(93) Crossley, S.; Faria, J.; Shen, M.; Resasco, D. E. *Science* **2010**, *327*, 68−72.
(94) Zapata, P. A.; Faria, J.; Pilar Ruiz, M.; Resasco, D. E. *Top. Catal.* **2012**, *55*, 38−52.
(95) Konwar, L.; Boro, J.; Deka, D. *Renew. Sust. Energy Rev.* **2014**, *29*, 546−564.
(96) Hara, M. *ChemSusChem* **2009**, *2*, 129−135.
(97) Takagaki, A.; Toda, M.; Okamura, M.; Kondo, J. N.; Hayashi, S.; Domen, K.; Hara, M. *Catal. Today* **2006**, *116*, 157−161.
(98) Hara, M. *Top. Catal.* **2010**, *53*, 805−810.
(99) Dawodu, F. A.; Ayodele, O.; Xin, J.; Zhang, S.; Yan, D. *Appl. Energy* **2014**, *114*, 819−826.
(100) Antunes, M. M.; Russo, P. A.; Wiper, P. V.; Veiga, J. M.; Pillinger, M.; Mafra, L.; Evtuguin, D. V.; Pinna, N.; Valente, A. A. *ChemSusChem* **2014**, *7*, 804−812.
(101) Budarin, V. L.; Clark, J. H.; Luque, R.; Macquarrie, D. J. *Chem. Commun.* **2007**, *6*, 634−636.
(102) Budarin, V. L.; Luque, R.; Macquarrie, D. J.; Clark, J. H. *Chem.—Eur. J.* **2007**, *13*, 6914−6919.
(103) Ren, H.; Yu, W. T.; Salciccioli, M.; Chen, Y.; Huang, Y. L.; Xiong, K.; Vlachos, D. G.; Chen, J. G. *ChemSusChem* **2013**, *6*, 798−801.
(104) Han, J. X.; Duan, J. Z.; Chen, P.; Lou, H.; Zheng, X. M. *Adv. Synth. Catal.* **2011**, *353*, 2577−2583.
(105) Han, J. X.; Duan, J. Z.; Chen, P.; Lou, H.; Zheng, X. M.; Hong, H. P. *Green Chem.* **2011**, *13*, 2561−2568.
(106) Qin, Y.; Chen, P.; Duan, J. Z.; Han, J. X.; Lou, H.; Zheng, X. M.; Hong, H. P. *RSC Adv.* **2013**, *3*, 17485−17491.
(107) Jongerius, A. L.; Bruijnincx, P. C. A.; Weckhuysen, B. M. *Green Chem.* **2013**, *15*, 3049−3056.
(108) Han, J. X.; Duan, J. Z.; Chen, P.; Lou, H.; Zheng, X. M.; Hong, H. P. *ChemSusChem* **2012**, *5*, 727−733.
(109) Ren, H.; Chen, Y.; Huang, Y. L.; Deng, W. H.; Vlachos, D. G.; Chen, J. G. *Green Chem.* **2014**, *16*, 761−769.
(110) Gosselink, R. W.; Stellwagen, D. R.; Bitter, J. H. *Angew. Chem., Int. Ed.* **2013**, *52*, 5089−5092.
(111) Elliott, D. C. *Energy Fuels* **2007**, *21*, 1792−1815.
(112) Ferrari, M.; Delmon, B.; Grange, P. *Carbon* **2002**, *40*, 497−511.
(113) Bui, V. N.; Laurenti, D.; Afanasiev, P.; Geantet, C. *Appl. Catal., B* **2011**, *101*, 239−245.
(114) Laurent, E.; Delmon, B. *Appl. Catal., A* **1994**, *109*, 77−96.
(115) Huber, G. W.; Iborra, S.; Corma, A. *Chem. Rev.* **2006**, *106*, 4044−4098.
(116) Lin, Y.-C.; Li, C.-L.; Wan, H.-P.; Lee, H.-T.; Liu, C.-F. *Energy Fuels* **2011**, *25*, 890−896.
(117) Gutierrez, A.; Kaila, R. K.; Honkela, M. L.; Slioor, R.; Krause, A. O. I. *Catal. Today* **2009**, *147*, 239−246.
(118) Laurent, E.; Delmon, B. *J. Catal.* **1994**, *146*, 281−291.
(119) Laurent, E.; Delmon, B. *Appl. Catal., A* **1994**, *109*, 97−115.
(120) Popov, A.; Kondratieva, E.; Goupil, J. M.; Mariey, L.; Bazin, P.; Gilson, J.-P.; Travert, A.; Maugèl, F. *J. Phys. Chem. C* **2010**, *114*, 15661−15670.
(121) Centeno, A.; Laurent, E.; Delmon, B. *J. Catal.* **1995**, *154*, 288−298.
(122) Ruiz, P. E.; Leiva, K.; Garcia, R.; Reyes, P.; Fierro, J. L. G.; Escalona, N. *Appl. Catal., A* **2010**, *384*, 78−83.
(123) Ferrari, M.; Maggi, R.; Delmon, B.; Grange, P. *J. Catal.* **2001**, *198*, 47−55.
(124) García, E.; Laca, M.; Pérez, E.; Garrido, A.; Peinado, J. *Energy Fuels* **2008**, *22*, 4274−4280.
(125) Sereshki, B. R.; Balan, S. J.; Patience, G. S.; Dubois, J. L. *Ind. Eng. Chem. Res.* **2010**, *49*, 1050−1056.
(126) Feng, Y.; Yang, Q.; Wang, X.; Liu, Y.; Lee, H.; Ren, N. *Bioresour. Technol.* **2011**, *102*, 411−415.
(127) Maris, E. P.; Davis, R. J. *J. Catal.* **2007**, *249*, 328−337.
(128) Li, B. D.; Wang, J.; Yuan, Y. Z.; Ariga, H.; Takakusagi, S.; Asakura, K. *ACS Catal.* **2011**, *1*, 1521−1528.
(129) Wu, Z. J.; Mao, Y. Z.; Wang, X. X.; Zhang, M. H. *Green Chem.* **2011**, *13*, 1311−1316.
(130) Jin, X.; Dang, L.; Lohrman, J.; Subramaniam, B.; Ren, S.; Chaudhari, R. V. *ACS Nano* **2013**, *7*, 1309−1316.
(131) Jin, X.; Roy, D.; Thapa, P. S.; Subramaniam, B.; Chaudhari, R. V. *ACS Sustainable Chem. Eng.* **2013**, *1*, 1453−1462.
(132) Sun, J.; Liu, H. *Green Chem.* **2011**, *13*, 135−142.
(133) Kirilin, A. V.; Hasse, B.; Tokarev, A. V.; Kustov, L. M.; Baeva, G. N.; Bragina, G. O.; Stakheev, A. Y.; Rautio, A.-R.; Salmi, T.; Etzold, B. J. M.; Mikkolaae, J.-P.; Yu, D. M. *Catal. Sci. Technol.* **2014**, *4*, 387−401.
(134) Sun, J.; Liu, H. *Catal. Today* **2014**, *234*, 75−82.
(135) Davis, S. E.; Ide, M. S.; Davis, R. J. *Green Chem.* **2013**, *15*, 17−45.
(136) Villa, A.; Schiavoni, M.; Campisi, S.; Veith, G. M.; Prati, L. *ChemSusChem* **2013**, *6*, 609−612.
(137) Wan, X.; Zhou, C.; Chen, J.; Deng, W.; Zhang, Q.; Yang, Y.; Wang, Y. *ACS Catal.* **2014**, *4*, 2175−2185.
(138) Guo, Z.; Liu, B.; Zhang, Q. H.; Deng, W. P.; Wang, Y.; Yang, Y. H. *Chem. Soc. Rev.* **2014**, *43*, 3480−3524.
(139) Prati, L.; Villa, A.; Lupini, A. R.; Veith, G. M. *Phys. Chem. Chem. Phys.* **2012**, *14*, 2969−2978.
(140) Purushothaman, R. K. P.; van Haveren, J.; van Es, D. S.; Melián-Cabrera, I.; Meeldijkc, J. D.; Heeres, H. J. *Appl. Catal., B* **2014**, *147*, 92−100.
(141) Pedersen, M.; Meyer, A. S. *New Biotechnol.* **2010**, *27*, 739−750.
(142) Bharadwaj, R.; Wong, A.; Knierim, B.; Singh, S.; Holmes, B. M.; Auer, M.; Simmons, B. A.; Adams, P. D.; Singh, A. K. *Bioresour. Technol.* **2011**, *102*, 1329−1337.
(143) Valdés-Solís, T.; Marbán, G.; Fuertes, A. B. *Microporous Mesoporous Mater.* **2001**, *43*, 113−126.
(144) Vergunst, T.; Kapteijn, F.; Moulijn, J. A. *Carbon* **2002**, *40*, 1891−1902.
(145) Park, J. H.; Xue, H.; Jung, J. S.; Ryu, K. *Korean J. Chem. Eng.* **2012**, *29*, 1409−1412.
(146) Kovalenko, G. A.; Perminova, L. V. *Carb. Res.* **2008**, *343*, 1202−1211.
(147) Nijhuis, T. A.; Beers, A.; Vergunst, T.; Hoek, I.; Kapteijn, F.; Moulijn, J. A. *Catal. Rev.* **2001**, *43*, 345−380.
(148) de Jong, K. P.; Geus, J. W. *Catal. Rev.* **2000**, *42*, 481−510.
(149) Zhao, X.; Lu, X.; Tze, W. T. Y.; Kim, J.; Wang, P. *ACS Appl. Mater. Interfaces* **2013**, *5*, 8853−8856.
(150) Gokhale, A. A.; Lu, J.; Lee, I. *J. Mol. Catal. B* **2013**, *90*, 76−86.
(151) Huang, R.; Qi, W.; Su, R.; He, Z. *Chem. Commun.* **2010**, *46*, 1115−1117.
(152) Huang, H.; Denard, C. A.; Alamillo, R.; Crisci, A. J.; Miao, Y.; Dumesic, J. A.; Scott, S. L.; Zhao, H. *ACS Catal.* **2014**, *4*, 2165−2168.
(153) Rinaldi, R.; Palkovits, R.; Schüth, F. *Angew. Chem., Int. Ed.* **2008**, *47*, 8047−8050.

(154) Liu, X.-Y.; Huang, M.; Ma, H.-L. Ma; Zhang, Z.-Q.; Gao, J.-M.; Zhu, Y.-L.; Han, X.-J.; Guo, X.-Y. *Molecules* **2010**, *15*, 7188−7196.
(155) Van Pelt, A. H.; Simakova, O. A.; Schimming, S. M.; Ewbank, J. L.; Foo, G. S.; Pidko, E. A.; Hensen, E. J. M.; Sievers, C. *Carbon* **2014**, *77*, 143−154.
(156) Onda, A.; Ochi, T.; Yanagisawa, K. *Top. Catal.* **2009**, *52*, 801−807.
(157) Shang, C.; Liu, Z.-P. *J. Am. Chem. Soc.* **2011**, *133*, 9938−9947.
(158) Nishimura, S.; Ikeda, N.; Ebitani, K. *Catal. Today* **2014**, *232*, 89−98.
(159) Job, N.; Heinrichs, B.; Ferauche, F.; Marien, J.; Pirard, J. P. *Proceedings of the International Symposium of Carbon for Catalysis*, Carbocat-2004, Lausanne, Switzerland, July 18−20, 2004. Abstract of Papers, pp 55−56
(160) Purnakala, V. S.; Figeuiredo, J. L. *Proceedings of the International Symposium of Carbon for Catalysis*, Carbocat-2004, Lausanne, Switzerland, July 18−20, 2004. Abstract of Papers, pp 51−52
(161) Moreno-Castilla, C.; Maldonado-Hódar, F. J.; Rivera-Utrilla, J.; Rodríguez-Castellón, E. *Appl. Catal., A* **1999**, *183*, 345−356.
(162) Maldonado-Hódar, F. J.; Moreno-Castilla, C.; Pérez-Cadenas, A. F. *Appl. Catal., B* **2004**, *54*, 217−224.
(163) Wu, J. C. S.; Lin, Z. A.; Tsai, F. M.; Pan, J. W. *Catal. Today* **2000**, *63*, 419−426.
(164) He, X.; Male, K. B.; Nesterenko, P. N.; Brabazon, D.; Paull, B.; Luong, J. H. T. *ACS Appl. Mater. Interfaces* **2013**, *5*, 8796−8804.
(165) Aravind, S. S. J.; Jafri, R. I.; Rajalakshmi, N.; Ramaprabhu, S. *J. Mater. Chem.* **2011**, *12*, 18199−18204.
(166) Boehm, H. P.; Mair, G.; Stoehr, T.; de Rincon, A. R.; Tereczki, B. *Fuel* **1984**, *63*, 1061−1063.
(167) Derbyshire, F.; de Beer, V. H. J.; Abotsi, G. M. K.; Scaroni, A. W.; Solar, J. M.; Skrovanek, D. J. *Appl. Catal.* **1986**, *27*, 117−131.
(168) Guerrero-Ruiz, A.; Rodriguez-Ramos, I.; Rodriguez-Reinoso, F.; Moreno-Castilla, C.; Lopez-Gonzalez, J. D. *Carbon* **1988**, *26*, 417−423.
(169) Sheng, Z.-H.; Gao, H.-L.; Bao, W.-J.; Wang, F.-B.; Xia, X.-H. *J. Mater. Chem.* **2012**, *22*, 390−395.
(170) Yang, Z.; Yao, Z.; Li, G.; Fang, G.; Nie, H.; Liu, Z.; Zhou, X.; Chen, X.; Huang, S. *ACS Nano* **2011**, *6*, 205−211.
(171) Qu, L.; Liu, Y.; Baek, J.-B.; Dai, L. *ACS Nano* **2010**, *4*, 1321−1326.
(172) Jeon, I.-Y.; Yu, D.; Bae, S.-Y.; Choi, H.-J.; Chang, D. W.; Dai, L.; Baek, J.-B. *Chem. Mater.* **2011**, *23*, 3987−3992.
(173) Wang, S.; Zhang, L.; Xia, Z.; Roy, A.; Chang, D. W.; Baek, J.-B.; Dai, L. *Angew. Chem., Int. Ed.* **2012**, *51*, 4209−4212.
(174) Dietrich, E.; Mathieu, C.; Delmas, H.; Jenck, J. *Chem. Eng. Sci.* **1992**, *7*, 3597−3604.
(175) Albal, R. S.; Shah, Y. T.; Schumpe, A.; Carr, N. L. *Chem. Eng. J.* **1983**, *27*, 61−80.
(176) Hsu, Y. C.; Peng, R. Y.; Huang, C. J. *Chem. Eng. Sci.* **1999**, *52*, 3883−3891.
(177) Mizan, J. L.; Morsi, B. I.; Chang, M. Y.; Maier, E.; Singh, C. P. P. *Chem. Eng. Sci.* **1994**, *49*, 821−830.